

MEASUREMENTS OF THE RELAXATION OF
QUASIPARTICLE BRANCH IMBALANCE
IN SUPERCONDUCTORS

John Clarke and James L. Paterson

November 1973

RECEIVED
LAWRENCE
RADIATION LABORATORY

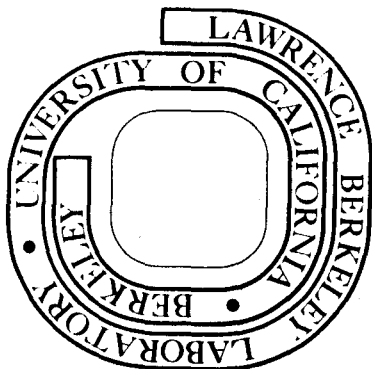
JAN 29 1974

LIBRARY AND
DOCUMENTS SECTION

Prepared for the U. S. Atomic Energy Commission
under Contract W-7405-ENG-48

TWO-WEEK LOAN COPY

This is a Library Circulating Copy
which may be borrowed for two weeks.
For a personal retention copy, call
Tech. Info. Division, Ext. 5545



DISCLAIMER

This document was prepared as an account of work sponsored by the United States Government. While this document is believed to contain correct information, neither the United States Government nor any agency thereof, nor the Regents of the University of California, nor any of their employees, makes any warranty, express or implied, or assumes any legal responsibility for the accuracy, completeness, or usefulness of any information, apparatus, product, or process disclosed, or represents that its use would not infringe privately owned rights. Reference herein to any specific commercial product, process, or service by its trade name, trademark, manufacturer, or otherwise, does not necessarily constitute or imply its endorsement, recommendation, or favoring by the United States Government or any agency thereof, or the Regents of the University of California. The views and opinions of authors expressed herein do not necessarily state or reflect those of the United States Government or any agency thereof or the Regents of the University of California.

Submitted to Journal of Low Temperature
Physics

LBL-2289
Preprint

UNIVERSITY OF CALIFORNIA

Lawrence Berkeley Laboratory
Berkeley, California

AEC Contract No. W-7405-eng-48

MEASUREMENTS OF THE RELAXATION OF QUASIPARTICLE BRANCH
IMBALANCE IN SUPERCONDUCTORS*

John Clarke⁺ and James L. Paterson⁺⁺

November 1973

Measurements of the Relaxation of Quasiparticle Branch
Imbalance in Superconductors*

John Clarke⁺ and James L. Paterson⁺⁺

Department of Physics, University of California
and
Inorganic Materials Research Division,
Lawrence Berkeley Laboratory,
Berkeley, California 94720

ABSTRACT

An imbalance Q in the quasiparticle populations of the $k > k_F$ and $k < k_F$ branches of a superconductor may be generated by the injection of a current through a tunnel barrier. This imbalance relaxes with a characteristic time τ_Q . The steady state value of Q gives rise to a quasiparticle potential V that differs from the pair chemical potential, and which may be measured by a second tunnel junction. Tinkham's theory of these effects is briefly reviewed. Detailed experimental results are presented for tin. Most of the data are for injection voltages much greater than the energy gap $\Delta(T)$. Close to the transition temperature T_c , Q relaxes by inelastic phonon

* This work was supported by the U.S. Atomic Energy Commission.

+ Alfred P. Sloan Foundation Fellow.

++ Present Address: Dept. of Physics, Univ. of Virginia, Charlottesville, Va. 22901

scattering, and $\tau_Q^{\text{ph}} = (1.0 \pm 0.2) \times 10^{-10} \Delta(0)/\Delta(T)$ sec. This time is about one-half that estimated by Tinkham. At temperatures somewhat below T_c , elastic scattering also contributes to the Q relaxation provided the superconducting energy gap is anisotropic. With a size effect limited mean free path of about 2800 Å, we find $\tau_Q^{\text{el}} \approx 1.4 \times 10^{-10}$ sec for $T/T_c < 0.6$, a value that is also in good agreement with Tinkham's theory. In a sample with a mean free path of 420 Å, and a greatly reduced anisotropy, τ_Q^{el} was increased to about 10^{-9} sec. Data were also taken for injection voltages close to $\Delta(T)/e$. The degree of imbalance per unit injection current was greatly reduced, as predicted by the theory. Preliminary measurements were made on lead. At 4.2K ($T/T_c = 0.58$), the characteristic time was about 3×10^{-12} sec. The quasiparticle potential apparently increased steadily as the temperature was lowered, probably indicating that the characteristic time also increased. This result is not well understood. However, it is possible that recombination processes play a role in the Q relaxation in lead.

1. INTRODUCTION

There has recently been considerable interest in the relaxation processes that occur in non-equilibrium superconductors. In particular, there have been a number of experiments¹⁻⁷ and theories^{1,8-12} concerned with effects that arise when the quasiparticles are not in thermal equilibrium with the Cooper pairs. It is now clear that there are at least two quite distinct non-equilibrium regimes, and we shall begin by briefly reviewing the basic concepts involved in these two situations.

When a superconductor is in thermal equilibrium, the chemical potential of a paired electron, μ_p , is equal to the chemical potential of a quasiparticle, μ_{qp} . The excitation spectrum of the quasiparticles is given by the BCS¹³ result $E_k = (\Delta^2 + \epsilon_k^2)^{1/2}$, where Δ is the energy gap and ϵ_k the one-electron energy, referred to the chemical potential. It is convenient to divide the quasiparticles into two branches, one for $k > k_F$ and one for $k < k_F$ (k_F is the Fermi wavevector): we shall label these branches $k_>$ and $k_<$ respectively. The reason for this division will emerge in due course. Within an accuracy of $\sim \Delta/E_F$, the number of $k_>$ quasiparticles per unit volume, $n_>$, is equal to the number of $k_<$ particles per unit volume, $n_<$.

In the first non-equilibrium regime, one generates an excess of quasiparticles over the equilibrium population, but the two quasiparticle branches remain equally populated ($n_> = n_<$). At the same time, the pair density is reduced. This situation can be induced, for example, by breaking pairs with either phonons or photons. Quasiparticles are generated with equal populations above and below the Fermi surface, so that no imbalance of the quasiparticle branches is created. The quasiparticles may be excited initially to energies $\gg \Delta$, especially if

optical photons are used. However, these quasiparticles rapidly decay into lower-lying energy states with phonon emission. The quasiparticles then recombine into pairs, with a recombination time, τ_R . For Al and Sn at all temperatures, and for Pb when $t = T/T_c \lesssim 0.4$, τ_R is much longer than the time taken by the quasiparticles to cool down to the lattice temperature (see Section 2.3 and Fig. 12). Thus the quasiparticle population comes into thermal equilibrium with the lattice, but not with the pairs. Under these conditions, one may define a quasiparticle chemical potential μ_{qp} , where μ_{qp} is greater than μ_p . The quasiparticle population is described by a Fermi function with energies referred to μ_{qp} rather than μ_p .¹¹ The recombination time is inversely proportional to the number of quasiparticles, and for $\Delta \gtrsim k_B T$ ($t \lesssim 0.9$) is of the form¹⁵ $\tau_R = \Gamma_R T^{-1/2} e^{\Delta/k_B T}$. As the temperature is increased from $t \sim 0.9$, τ_R reaches a minimum value, and then increases again close to T_c . For Pb above $t \sim 0.4$, τ_R is shorter than the cooling time. The quasiparticles recombine as they cool down, and it is not appropriate to define a quasiparticle chemical potential.

When the quasiparticles cool and recombine, they emit phonons. Phonons with energy $\geq 2\Delta$ have a non-zero probability of pair breaking and thereby further increasing the quasiparticle population. For this reason the effective¹⁵ decay time, τ_R^{eff} , of a non-equilibrium quasiparticle population (with $n_{>} = n_{<}$) may be very much greater than τ_R . τ_R^{eff} has been measured in thin superconducting films in which an excess quasiparticle population is generated by tunnel injection,¹⁶⁻¹⁹ or by phonon²⁰ or photon⁶ excitation. The steady state population is measured by

means of a tunnel junction between the superconductor and a second superconducting film. The excess population increases the quasiparticle current flowing through this junction at voltages below the sum of the energy gaps of the two superconductors. It is often difficult to deduce an accurate value of τ_R from τ_R^{eff} : the enhancement depends critically upon the nature of the substrate and the coupling of the films to the substrate and the helium bath. Gray, Long, and Adkins¹⁸ found $\Gamma_R(\text{Al}) = 2.8 \times 10^{-8} \text{ sec K}^{1/2}$, in good agreement with the calculated value of Gray.²¹ Eisenmenger²⁰ found $\Gamma_R^{\text{eff}}(\text{Sn}) \approx 5 \times 10^{-10} \text{ sec K}^{1/2}$, while Parker and Williams,⁶ and Parker²² estimated $\Gamma_R^{\text{eff}}(\text{Sn}) \approx 2 \times 10^{-9} \text{ sec K}^{1/2}$, and $\Gamma_R^{\text{eff}}(\text{Pb}) \approx 2 \times 10^{-12} \text{ sec K}^{1/2}$. There appears to be no theoretical value for $\Gamma_R(\text{Sn})$, while the measured value of $\Gamma_R^{\text{eff}}(\text{Pb})$ is about a factor of 7 greater than the theoretical estimate of Rothwarf and Cohen²³ for $\Gamma_R(\text{Pb})$.

The non-equilibrium situation with $n_{>} = n_{<}$ was studied in a rather different type of experiment by Testardi,² who generated quasiparticles in thin superconducting films by means of a pulsed laser. He found that the films could be driven normal by a sufficiently powerful laser pulse, and showed that the effect was not merely due to lattice heating. Owen and Scalapino¹¹ showed that the excess quasiparticle population generated by the photons reduced the energy gap at a given temperature, and that the transition temperature was therefore lowered. Parker and Williams⁶ were able to confirm the dependence of Δ on the excess quasiparticle population by studying the I-V characteristic of an SIS tunnel junction irradiated with a laser (it was in this way that they estimated τ_R^{eff} for Pb and Sn). They were also able to deduce the dependence of μ_{qp} on the excess number of quasiparticles, and found excellent agreement with the theory of Owen and Scalapino.

It appears that the general concepts involved in this kind of pair-quasiparticle non-equilibrium are well understood, although only τ_R (A1) is known with any great precision. However, more accurate values for Sn and Pb will probably be available in the near future.²²

In the second non-equilibrium regime, an imbalance is generated in the $k_>$ and $k_<$ quasiparticle populations, illustrated in Fig. 1. We define the imbalance per unit volume as $Q = n_> - n_<$. This imbalance implies that a quasiparticle current is flowing. Q relaxes in a characteristic time τ_Q , the branch mixing time, through the scattering or creation of a quasiparticle from one branch to the other or through the annihilation / of two quasiparticles on the same branch. We shall see that for Sn, τ_Q is much smaller than τ_R . Thus if an excess of (say) $k_>$ quasiparticles is suddenly created, Q will relax in a time τ_Q to a $Q = 0$ distribution in which there is still an excess number of quasiparticles ($\mu_{qp} > \mu_p$). This excess will subsequently decay in a time τ_R^{eff} . It will also be seen that close to T_c , each quasiparticle branch will come separately into internal thermal equilibrium before very much branch mixing can occur. In this situation, we can define chemical potentials for each branch, $\mu_>$ and $\mu_<$, which will differ when $Q \neq 0$. For Pb when $t \gtrsim 0.4$, τ_R is comparable to or less than τ_Q . Recombination may then become the dominant Q relaxation processes.

The fact that a non-zero Q implies the existence of a quasiparticle current in the superconductor was demonstrated by Pippard, Shepherd, and Tindall.¹ They measured the resistances of superconductor-normal metal-superconductor sandwiches and of superconducting cylinders in the

intermediate state. In both types of sample, they found the resistance was independent of temperature at low reduced temperatures, but increased substantially as the temperature was raised towards the transition temperature. This increase was ascribed to an additional resistance in the superconductor near the interface. At low reduced temperatures, quasiparticles incident on the interface from the normal side have energies much less than Δ , and are Andreev²⁴ reflected. In this process, a quasiparticle above the Fermi surface is reflected as one below the Fermi surface, while a pair propagates into the superconductor. Thus the conversion from normal current to supercurrent occurs at the NS interface.²⁵ At higher temperatures ($k_B T \gtrsim \Delta$), a fraction of the quasiparticles propagate into the superconductor, and in the presence of a current, have a $Q \neq 0$ distribution. This quasiparticle current decays in the superconductor as Q decays, over a characteristic length¹ $\lambda_Q = \tau_Q v_F$ in the clean limit or $\lambda_Q = (\ell v_F \tau_Q / 3)^{1/2}$ in the dirty limit (ℓ is the mean free path in the superconductor). The quasiparticle current in the superconductor dissipates power, and this dissipation is manifested as an interface resistance. As the temperature is raised, more quasiparticles propagate into the superconductor and the boundary resistance increases. The quasiparticle current is maintained by an electric field which also decays exponentially from the interface into the superconductor with the characteristic length λ_Q . As we shall see later, this "quasiparticle potential" at any point is related to, but not directly proportional to Q . (Pippard et al.¹ assumed that the potential was zero in the superconductor and discontinuous at the interface. It now seems clear that there is no discontinuity, and that the potential decays smoothly into the superconductor.)

Subsequently, Clarke⁴ measured the quasiparticle potential directly. A current through an Al-AlOx-Sn tunnel junction biased at a voltage

$\gg \Delta_{\text{Sn}}/e$ generated a branch imbalance in the superconducting Sn. The resulting quasiparticle potential was measured by a second tunnel junction (Sn-SnOx-Cu) grown on top of the Sn. The quasiparticle potential was measured between the Cu and a point on the Sn strip far ($\gg \lambda_Q$) from the non-equilibrium region. A theory of the mechanisms involved was developed by Tinkham and Clarke,¹⁰ and in more detail by Tinkham.¹² The theory indicated that inelastic scattering led to branch mixing at all temperatures, and that a significant contribution from elastic scattering would occur at temperatures well below T_c if the energy gap were anisotropic or spatially non-uniform. In the relatively dirty Sn films used in the experiment, the inelastic processes were dominant at all temperatures, and the preliminary value²⁶ of τ_Q was $\sim 3 \times 10^{-10} \Delta(0)/\Delta(T)$ sec. The theoretical value for τ_Q (due to phonon processes only) was $\sim 2 \times 10^{-10} \Delta(0)/\Delta(T)$.

The experiment performed by Clarke was stimulated by a theory of Rieger, Scalapino, and Mercereau,⁹ who used time-dependent Ginzburg-Landau theory to discuss the second non-equilibrium regime. Their theory predicted qualitatively the observed effects, but being a phenomenological theory, could not account for the detailed microscopic processes. Thus their work does not contain the ideas of branch imbalance or of $\mu_{>} \neq \mu_{<}$: however, their results have the same form as the work of Pippard et al.¹ and Tinkham and Clarke¹⁰ except in that they involve the Ginzburg-Landau time τ_{GL} rather than τ_Q , and the coherence length ξ_{GL} rather than λ_Q . A phenomenological theory by Putterman and Ouboter⁷ also pointed out that a divergence in the supercurrent (which must exist when a quasiparticle current is converted into a supercurrent) implied dissipation in the superconductor.

This paper extends the earlier work of Clarke⁴ on the measurement of τ_Q in Sn, and also reports preliminary work on Pb. In Section 2 we summarize the salient points of the theory^{10,12}: the distribution of the injected quasiparticles, the nature of the quasiparticle potential, and the cooling and branch mixing of the injected quasiparticles. Section 3 deals with the experimental configuration and measurements. In Sections 4 and 5, we present the experimental results and their interpretation for Pb and Sn. Section 6 contains a summary, and suggestions for further work.

2. THEORY

A suitable configuration for the generation and detection of a quasiparticle branch imbalance Q is shown in Fig. 2. A current I flows through the NIS injection junction of area w^2 , and creates a branch imbalance in the non-equilibrium volume $\Omega = w^2 d$ of the superconductor S , where d is the film thickness. Provided that $\lambda_Q \gg d$, Q is spatially uniform across the film, and provided that $w \gg \lambda_Q$, the non-equilibrium volume is accurately given by Ω , with negligible edge corrections. A current of either polarity increases the number of quasiparticles in Ω , and thus decreases the number of pairs. This pair reduction has the effect of reducing k_F . However, pairs flow into Ω from the remainder of the superconductor, and create a space charge so that the electrochemical potential of the pairs (which includes the electrostatic potential) is restored throughout S to its equilibrium value, μ_p . We refer all voltages to μ_p . At distances much greater than λ_Q from the non-equilibrium

region, all chemical potentials will have their equilibrium values:

$\mu_p = \mu_{qp} = \mu_> = \mu_<$. The quasiparticle potential V (Fig. 2) is measured by a normal probe N_p coupled to Ω via a second tunnel junction. The quasiparticle potential V is then defined as the potential between N_p and S with zero current flowing through N_p . The injection and detection tunnel junctions avoid complications due to the proximity effect,²⁷ that is, a depression of Δ in S , and a tendency for the pairs to leak into the normal metals, thereby making Ω an imprecisely defined volume.

The calculation of V may be conveniently divided into several parts, which we now briefly review. First, we consider the creation of the branch imbalance by the injection current, second the quasiparticle potential V detected by the normal probe junction for a given branch imbalance, and third the cooling of the injected quasiparticles and the relaxation of Q . The various calculations have been given by Tinkham and Clarke,¹⁰ and by Tinkham,¹² and we shall merely summarize the results for comparison with experiment.

2.1 Tunnel Injection

The quasiparticle population²⁸ of Ω is increased for both electron injection into S and electron extraction from S . Figure 3(a) shows electron injection: the electron has a probability $u_{k>}^2$ of entering the $k_>$ branch, and a probability $u_{k<}^2 = v_{k>}^2$ of entering the $k_<$ branch. The coherence factors have their usual definition,¹³ $u_k^2(\epsilon_k) = \frac{1}{2}(1 + \epsilon_k/E_k) = v_k^2(-\epsilon_k)$, and $v_k^2(\epsilon_k) = \frac{1}{2}(1 - \epsilon_k/E_k) = u_k^2(-\epsilon_k)$. If the bias voltage of the tunnel junction V_{inj} is much larger than Δ/e and $k_B T/e$, the injected quasiparticles are distributed in energy from Δ to eV_{inj} . However, for most of these quasiparticles, $u_{k>}^2 \gg u_{k<}^2$; thus

the majority of the quasiparticles are on the $k_>$ branch rather than the $k_<$ branch. On the other hand, if $eV_{inj} \sim \Delta$, $u_{k>}^2 \sim u_{k<}^2$, and the branches are more equally populated: the resulting Q is therefore small. Fig. 3(b) shows the situation for electron extraction, a process that again involves two channels. A pair above or below the Fermi surface (with relative probabilities $v_{k>}^2$ and $v_{k<}^2$) breaks up to form an excitation in S , and also to inject an electron into N . For $V_{inj} \gg \Delta/e$, $v_{k<}^2 \gg v_{k>}^2$, and the $k_<$ branch is preferentially populated.

The branch imbalance per unit volume, Q , is defined as

$$Q = n_> - n_< = 2N(0) \int_{\Delta}^{\infty} \mathcal{N}(E) (f_{k>} - f_{k<}) dE, \quad (1)$$

where $N(0)$ is the density of states per spin in the superconductor at the Fermi surface, $\mathcal{N}(E) = E/(E^2 - \Delta^2)^{1/2}$ is the normalized BCS¹³ density of states, and $f_{k>}$ and $f_{k<}$ are the steady-state non-equilibrium populations of the $k_>$ and $k_<$ branches. We wish to calculate Q as a function of the tunnel injection current, I , the injection voltage, V_{inj} , and the temperature T .

The steady state value of Q is just $\dot{Q}_{inj} \tau_Q$ where \dot{Q}_{inj} is the rate at which Q is created by the injection current. Tinkham¹² has shown that in the limit $V \ll V_{inj}$ (typically, $V \sim nV$ whereas $V_{inj} \sim mV$), \dot{Q}_{inj} is given by

$$\dot{Q}_{inj} = \frac{G_{NN}}{e^2 \Omega} \int_{\Delta}^{\infty} [f(E - eV_{inj}) - f(E + eV_{inj})] dE, \quad (2)$$

where G_{NN} is the tunneling conductance with the superconductor in the normal state, and f is the Fermi function. $\dot{Q}_{inj} \Omega$ differs from the injection current

$$\frac{I}{e} = \frac{G_{NN}}{e^2} \int_{\Delta}^{\infty} \mathcal{N}(E) [f(E - eV_{inj}) - f(E + eV_{inj})] dE, \quad (3)$$

only by a factor of $\mathcal{N}(E)$. The value of Q_{inj} for a given injection current depends upon V_{inj} , through the energy dependences of the u_k and v_k . Following Tinkham,¹² we introduce the parameter $F(V_{inj}, T) = \Omega e Q_{inj} / I$ which characterizes the degree of imbalance of the injected population:

$$F = \frac{\int_{\Delta}^{\infty} [f(E - eV_{inj}) - f(E + eV_{inj})] dE}{\int_{\Delta}^{\infty} \mathcal{N}(E) [f(E - eV_{inj}) - f(E + eV_{inj})] dE} \leq 1. \quad (4)$$

F has been calculated numerically and is plotted vs eV_{inj}/Δ for several values of $\Delta/k_B T$ in Fig. 4(a). Fig. 4(b) shows F vs $eV_{inj}/\Delta(0)$ for the corresponding values of the reduced temperature t . For $eV_{inj} \gg \Delta$ virtually all of the quasiparticles are created on one branch (the $k_>$ branch for electron injection or the $k_<$ branch for electron extraction) and $F \approx 1$. For $eV_{inj} \leq \Delta$ there are two regimes, $k_B T \gg \Delta$ and $k_B T \ll \Delta$. For $k_B T \gg \Delta$ most of the electrons enter the superconductor at energies high relative to Δ , and F remains close to unity. For $k_B T \ll \Delta$ the electrons are injected into states near Δ where $u_{k>}^2 \approx u_{k<}^2$, and F goes to zero. The quantity F has the limiting forms (given by Tinkham¹²)

$$F = \begin{cases} 2f(\Delta)/g_{NS} & (eV_{inj} \ll k_B T, \text{ all } T) \quad (5a) \\ 1 & (T \approx T_c, \text{ all } V_{inj}) \quad (5b) \\ \left(\frac{eV_{inj} - \Delta}{eV_{inj} + \Delta} \right)^{1/2} & (T = 0, \text{ all } V_{inj}) \quad (5c) \\ 1 & (eV_{inj} \gg \Delta, \text{ all } T), \quad (5d) \end{cases}$$

where $g_{NS} = G_{NS}/G_{NN}$ is the normalized conductance of an ideal NIS tunnel junction in the appropriate limit (g_{NS} has been tabulated by Bermon²⁹).

Finally, the steady state value of Q as a function of I and F is given by

$$Q = Q_{inj} \tau_Q = F(V_{inj}, T) I \tau_Q / \Omega e. \quad (6)$$

In the limit $eV_{inj} \gg \Delta$ in which the experiments of Clarke⁴ were performed, $F \approx 1$ for all temperatures, and a good approximation to Eq. (6) is

$$Q = I \tau_Q / \Omega e. \quad (eV_{inj} \gg \Delta). \quad (7)$$

We next calculate the dependence of the quasiparticle potential V upon the steady state value of Q .

2.2 Detection of Quasiparticle Imbalance

Consider the configuration of Fig. 2 with the leads marked V shorted together. Thus the normal probe is clamped at μ_p (we assume the probe resistance to be negligible compared with the probe junction resistance.) In the presence of a quasiparticle imbalance in Ω , the current that flows through the probe junction can be shown to be^{10,12}

$$I_p (V = 0) = \frac{G_{NN}}{e} \int_0^\infty (f_{k<} - f_{k>}) dE = - \frac{G_{NN} Q^*}{2N(0)e}, \quad (8)$$

where

$$Q^* = 2N(0) \int_\Delta^\infty (f_{k>} - f_{k<}) dE, \quad (9)$$

and G_{NN} now refers to the probe junction. The quantity Q^* differs from

Q [Eq. (1)] only by the absence of the normalized superconducting density of states $\mathcal{N}(E)$.

We now insert a voltage source between the leads marked V in Fig. 2. The quasiparticle potential V is defined as the external voltage V ($\ll k_B T/e$) required to reduce $I_p(V=0)$ to zero:

$$V = - I_p(V=0)/G_{NS} = Q^*/2N(0)eg_{NS}(0), \quad (10)$$

where $g_{NS}(0) = G_{NS}/G_{NN}$ is the normalized conductance of the probe junction in the limit $V \rightarrow 0$.

Eq. (10) relates V to Q^* , whereas Eq. (6) is an expression for Q rather than Q^* . We can combine these two equations to obtain

$$V = F \frac{Q^*}{Q} \frac{I\tau_Q}{2N(0)e^2\Omega g_{NS}(0)}. \quad (11)$$

In principle, if we measure V as a function of I , we can derive a value for τ_Q . The factor $F \leq 1$ represents the degree of branch imbalance of the injected quasiparticles, and can be calculated from the known values of V_{inj} and T . The factor Q^*/Q reflects the fact that the probe junction measures Q^* rather than Q . At temperatures much below T_c , it is difficult to make very accurate estimates of Q^*/Q , but, as we shall see in the next section, near T_c , $Q^*/Q \approx 1$. Thus the best estimates of τ_Q are obtained near T_c , where $Q^*/Q \approx 1$, and for $eV_{inj} \gg \Delta$, when $F \approx 1$.

In these limits Eq. (11) reduces to

$$V = \frac{I\tau_Q}{2N(0)e^2\Omega_{g_{NS}}(0)} \quad (T \sim T_c, eV_{inj} \gg \Delta). \quad (12)$$

It should be emphasized that the quasiparticle potential is measured with zero current flowing through the probe junction. This zero-current measurement is quite different from the determination of τ_R mentioned in Section 1, in which the detection junction is current biased at a voltage many orders of magnitude greater than the quasiparticle potential.

In the following section, we discuss the parameters which determine τ_Q .

2.3 Cooling of Injected Quasiparticles and Relaxation of Q

The quasiparticles generated in the superconductor by tunnel injection are in general at high energies relative to both Δ and $k_B T$. Consequently, they begin to cool very rapidly towards the sample temperature by phonon emission. The details of this non-equilibrium process are complicated, but Tinkham¹² has performed a model calculation to obtain an estimate of the cooling time. He characterizes the quasiparticle population by a mean energy $k_B T^*$, and finds a cooling law in which $T^* \propto (\text{time})^{-1/3}$. If the sample temperature is much less than T_c , the time for the injected quasiparticles to cool down to T_c is given by

$$t(T_c) \approx 0.19 \tau_\theta (\theta/T_c)^3 \quad (T \ll T_c), \quad (13)$$

where τ_θ is the electron scattering time due to phonon processes at the Debye temperature θ . For $T \approx T_c$, $t(T_c)$ will be somewhat longer. Thus $t(T_c)$ gives a rough estimate of the time

taken for the quasiparticles to come into thermal equilibrium with the lattice. This estimate is probably accurate to within a factor of 2. This cooling time is comparable¹² in magnitude with the phonon scattering time for an electron at the Fermi surface when the sample is in thermal equilibrium at T_c , $0.12 \tau_\theta (\theta/T_c)^3$. It would therefore seem that $t(T_c)$ provides a reasonable estimate of the quasiparticle cooling time to a mean energy $k_B T_c$ for all lattice temperatures up to T_c , regardless of how high the injection energy is. For Sn ($\tau_\theta = 2 \times 10^{-14}$ sec, $\theta = 200\text{K}$, $T_c = 3.8\text{K}$ for a thin film), $t(T_c) \approx 5.5 \times 10^{-10}$ sec. For Pb ($\tau_\theta = 3 \times 10^{-14}$ sec, $\theta = 105\text{K}$, $T_c = 7.2\text{K}$), $t(T_c) \approx 1.8 \times 10^{-11}$ sec.

Having given some estimate for the time required for the quasiparticles to cool down, we now consider the mechanisms involved in the relaxation of the branch imbalance.^{10,12} In general, this relaxation can occur through both inelastic (phonon) and elastic scattering, and we shall discuss first the inelastic case. Q can relax by the scattering of an excitation from one branch to the other, a process governed by a coherence factor $(uu' - vv')^2$, or by the annihilation or creation of a pair of excitations on the same branch, the coherence factor being $(vu' + uv')^2$. Each of these processes changes Q by 2. A consideration of the coherence factors reveals that significant Q relaxation occurs only when either the initial or final energy lies between Δ and $\sim 2\Delta$. Near T_c , when $\Delta \ll k_B T$, only a fraction $\sim \Delta/k_B T \ll 1$ of the quasiparticles lies in this range, and we therefore might expect τ_Q to be proportional to $1/\Delta$. We shall see that sufficiently close to T_c , τ_Q is long compared with $t(T_c)$, so that each quasiparticle branch comes separately into thermal equilibrium before

significant Q relaxation occurs. In that case, the population of each branch may be described by a Fermi function f_k referred to a chemical potential $\mu_>$ or $\mu_<$. For each branch, the perturbation of the population from the equilibrium population is $\delta f_k = + (\partial f_k / \partial E_k) \delta \mu$, where $\delta \mu$ is the displacement of the chemical potential from μ_p . If we insert the expressions for $\delta f_{k>} - \delta f_{k<} = f_{k>} - f_{k<}$ in Eqs. (9) and (10), we find $V = (\mu_> - \mu_<) f(\Delta) / e g_{NS}(0)$. Further, for the same limit in which the chemical potentials can be defined, the same substitutions in Eqs. (1) and (9) yield $Q^*/Q = 2f(\Delta) / g_{NS}(0) \approx 1$. Therefore near T_c we find

$$V = (\mu_> - \mu_<) / 2e. \quad (T \sim T_c). \quad (14)$$

Thus $V = 0$ if $\mu_> = \mu_<$, even if both chemical potentials differ from μ_p . This result emphasizes that it is essential to have a branch imbalance to obtain a non-zero quasiparticle potential.

Tinkham¹² has estimated the contribution of inelastic scattering to τ_Q near T_c by including both branch crossing and the annihilation and creation of pairs of quasiparticles, and finds

$$\tau_Q^{ph} = 0.068 \tau_\theta \left(\frac{\theta}{T_c}\right)^3 \left(\frac{\Delta(0)}{\Delta(T)}\right). \quad (T \sim T_c). \quad (15)$$

This estimate is expected to be accurate to within a factor of 2. For Sn and Pb, the values of $0.068 \tau_\theta (\theta/T_c)^3$ are about 2×10^{-10} sec and 6×10^{-12} sec respectively.

At temperatures well below T_c , Q and T^* relax at similar rates (i.e. $\tau_Q \lesssim t(T_c)$), and the assumption that the branches reach separate

internal equilibrium before Q relaxes is no longer valid. Tinkham has also considered this case, and finds an expression for τ_Q^{ph} identical in form to Eq. (15), but with a prefactor of 0.044 rather than 0.068. The accuracy of the theory in this region is thought to be much lower.

We consider next Q relaxation by elastic scattering. These processes are governed by the coherence factor $(uu'-vv')^2$. We notice first that for an isotropic, spatially uniform superconductor, $(uu'-vv')^2$ is zero for k and k' on different branches, since $E = E'$ and $\Delta = \Delta'$. However, for an anisotropic superconductor, the coherence factor is non-zero, since $E = E'$, but $\Delta \neq \Delta'$, and elastic scattering induces branch mixing. The detailed behavior of these processes is again complicated, and has been discussed by Phillips.³⁰ Tinkham¹² estimates the branch mixing time due to elastic scattering to be

$$\tau_Q^{\text{el}} = \frac{\tau_1}{\langle a^2 \rangle_0} \left[1 + \left(\frac{\hbar}{2\tau_1\Delta} \right)^2 \right] \left(\frac{k_B T^*}{\Delta} \right) \left(1 + \frac{k_B T^*}{\Delta} \right), \quad (16)$$

where τ_1 is the elastic scattering time, and $\langle a^2 \rangle_0$ is the mean square anisotropy³¹ in Δ . The factor $[1 + (\hbar/2\tau_1\Delta)^2]$ estimates the reduction in the anisotropy due to Anderson³² averaging. In Tinkham's paper,¹² this factor appeared squared, but the linear term seems to be more consistent with the calculation of Markowitz and Kadanoff,³¹ and is also in tolerable agreement with the experimental results of Claiborne and Einspruch³³ for Sn. For the present purpose, we feel that $\langle a^2 \rangle = \langle a^2 \rangle_0 / [1 + (\hbar/2\tau_1\Delta)^2]$ is probably an adequate representation of the dependence of $\langle a^2 \rangle$ on temperature and mean free path. Notice that near T_c , T^* is never less than T_c , and τ_Q is proportional to Δ^{-4} . The phonon processes will therefore dominate in this temperature range. At low temperatures, whether or not the anisotropic scattering

contributes significantly to the overall branch relaxation depends on the dirtiness of the superconductor.

From Eq. (16), we see that τ_Q^{el} has a minimum with respect to τ_1 when $\tau_1 = \hbar/2\Delta$. This condition can be rewritten as $\ell = \pi\xi(T)/2$, where $\ell = \tau_1 v_F$ is the mean free path for elastic scattering, and $\xi(T) = \hbar v_F / \pi\Delta$. The minimum value is

$$\tau_Q^{el}(\min) = \frac{2\tau_1}{\langle a^2 \rangle_0} \left(\frac{k_B T^*}{\Delta} \right) \left(1 + \frac{k_B T^*}{\Delta} \right). \quad (17)$$

For $\ell < \pi\xi(T)/2$, τ_Q^{el} increases as ℓ decreases: the anisotropy decreases faster than the scattering rate ($\propto \ell^{-1}$) increases. For $\ell > \pi\xi(T)/2$, τ_Q^{el} increases as ℓ increases: the scattering rate increases more rapidly than the anisotropy increases.

The biggest uncertainty in Eqs. (16) and (17) is the value of T^* . We shall make an experimental estimate of T^* in Section 4.

Another possible contribution to elastic branch mixing arises from the spatial inhomogeneity of Δ close to the surfaces of the films.³⁴

We have not estimated the branch mixing rate for this mechanism.

Experimentally, it may be difficult to distinguish between these processes and the anisotropic processes.

3. EXPERIMENTAL METHODS

3.1 Sample Preparation for Sn Samples

The experimental realization of the configuration of Fig. 2 is shown in Fig. 5. Four such samples of a given thickness of Sn were prepared simultaneously on a glass microscope slide. The Al-AlO_x-Sn tunnel junctions were made by first evaporating a 3 mm wide Al strip XX', 1200 Å to 2000 Å thick, onto the substrate and immediately exposing the film to a one atmosphere mixture of air and nitrogen for a few minutes. The chamber was then evacuated and a 3 mm wide cross strip of Sn YY' of the required thickness deposited. For sample 19 the electronic mean free path in the Sn was reduced by the addition of 3 wt% of In: ^{was} the film/produced by flash evaporation of small pellets of the alloy. At this point, the samples were removed from the evaporator and the junction resistances measured. Resistances of approximately 0.5 Ω were most desirable. These resistances increased to 1 to 2 Ω in the four hours or so required to complete the samples and cool them to liquid nitrogen temperatures.

For all but one of the sets of samples the Sn was exposed to air for 20 to 150 minutes to produce a thin oxide barrier. The slide was returned to the evaporator and two 500 Å thick layers of SiO were used to mask off all but an area of $9.4 \times 10^{-3} \text{ cm}^2$ in the center of the tunnel junction. A strip of CuAl approximately 2 μm thick was then deposited diagonally so as to make contact with the Sn oxide through the window in the SiO. The CuAl served as the normal probe. The resistance of this strip, typically 1Ω, would have severely impaired the voltage resolution. For this reason, a Pb strip ZZ' was evaporated over the

CuAl to reduce the lead resistance of the probe to $\sim 5 \times 10^{-7} \Omega$, the resistance of the 2 μm thick layer in the window area. The completed normal probe thus consisted of a superconductor-insulator-normal metal-superconductor junction. The Al (3 wt%) was added to the Cu to reduce the electron mean free path to $\sim 100 \text{ \AA}$. This in turn reduced the pair decay depth in the CuAl and precluded pair current flow through the junction.

The set of samples 11 was made without exposing the Sn strip to air. After completion of the tunnel junctions, the SiO and the CuAl were deposited. For these samples, the CuAl was therefore in good electrical contact with the Sn.

The thickness of each film was monitored during evaporation by a quartz crystal microbalance. After completion of the low temperature measurements, the thickness of the Sn strips was remeasured with a Varian \AA -scope interferometer. The quoted thicknesses of Sn have an accuracy of $\pm 100 \text{ \AA}$.

3.2 Sample Preparation for Pb Samples

We also made two sets of samples (12,16) in which the superconductor was Pb. The preparations followed the same procedure as that for the Sn samples. However, the resistance of the Al-AlOx-Pb junctions was found to decrease with time at room temperature. For this reason, the desired initial resistance of the junctions was $\sim 2 \Omega$.

3.3 Electrical Measurements

The Sn (or Pb)-oxide-CuAl-Pb junctions of the four samples on each slide were connected in series with a known resistance (R_{std}) and a superconducting galvanometer. The galvanometer consisted of a superconducting

coil inserted into a Develco SQUID (Fig. 5). The output from the SQUID was detected, amplified, and fed back as a current I_F into the standard resistance. The closed-loop SQUID voltmeter circuit has been discussed in detail by Giffard et al.³⁵ and by Clarke.³⁶ Any voltage appearing between the normal probe and the superconductor was thus measured with zero current flowing in the circuit, the voltage being equal to $I_F R_{\text{std}}$. Two standard resistances were used. The first consisted of a 1 cm length of copper wire to which superconducting leads had been attached; its resistance was $0.160 \mu\Omega$. The second consisted of a 1 cm square of manganin 0.025 cm thick,³⁵ part of each face being coated with solder; its resistance was $2.54 \mu\Omega$. The entire low temperature circuit was immersed in liquid helium.

The circuit was carefully shielded to minimize the effects of changing external fields, and of vibrations in static fields. The earth's field was reduced to a few tens of mG by means of two concentric mu-metal shields surrounding the cryostat. The remnant flux was then stabilized by a superconducting lead can surrounding the low temperature circuit. The effective coupling area of the circuit was minimized by taping it (including the glass slide) to a sheet of lead, thus reducing spurious signals due to vibration of the loop in the ambient magnetic field, and due to external fields coupled into the loop.

Above the λ -point, the noise in the circuit was considerably above Johnson noise. We attribute the excess noise to thermoelectric voltages generated in the standard resistor.³⁵ The noise in the band from 0 to 1 Hz at 2.5K was typically 2×10^{-13} V for the copper standard, and 10^{-12} V for the manganin standard. This excess noise vanished abruptly

as the temperature of the helium bath was lowered through the λ -point. At temperatures below the λ -point, the limiting noise was the Johnson noise generated in the probe junctions and the standard resistor.

Each specimen on the slide was examined independently by applying a current to the appropriate terminals. The following three parameters were measured. First, the current-voltage characteristic of the injection junction was plotted on an X-Y recorder by applying a current to X'Y' and measuring the voltage across XY. Second, the probe resistance was determined by applying a current to Y'Z' and measuring the voltage which appeared across YZ by means of the SQUID circuit. Third, the non-equilibrium voltage V appearing across YZ was measured with the SQUID circuit as a function of the injection current I. This I-V characteristic was also plotted on the X-Y recorder.

4. EXPERIMENTAL RESULTS: Sn

This section deals with the injection and probe junctions, the determination of τ_Q , and the voltage and temperature dependences of F.

In Table I we list various electronic parameters for Sn and Pb used in the calculations.

4.1 The Injection Junction

The injection junctions were high quality Al-AlOx-Sn tunnel junctions. The resistance of the Al strip was $\sim 0.1 \Omega$ per square at 4.2K. We could therefore use junctions with resistances as low as 1Ω and still have the injection current density uniform to $\sim 10\%$. These low resistance junctions permitted us to use high injection currents and so obtain correspondingly high non-equilibrium voltages in the region of special

interest, $0 < eV_{inj} < \Delta$. The I-V characteristic for each sample was plotted at each temperature; the low voltage portion was expanded and the slope dI/dV measured in the limit $eV_{inj} \rightarrow 0$. The normalized conductance $g_{NS}(0)$ was determined, and compared with the theoretical prediction.²⁹ The agreement was generally excellent. Data were rejected from samples in which the injection junctions had excess currents.

4.2 Probe Junction

The normal probe consisted of a Sn-SnOx-CuAl junction in series with the "lead" resistance of the CuAl. The resistance of the CuAl ($\sim 5 \times 10^{-7} \Omega$) was about 5% of the junction resistance at T_c (Sn), typically $10^{-5} \Omega$. From the variation of the probe resistance with temperature, we computed values for $g_{NS}(0)$, which were subsequently used in deriving a value for τ_Q .

Since the voltage across the probe junctions was typically 10^{-9} V or less, the measured normalized conductance could be compared with that for an ideal NIS junction²⁹ in the low voltage limit $eV \ll \Delta$. This comparison is made in Fig. 6: each set of points represents an average over all the acceptable samples for a given thickness of Sn. In general, there was a large spread in the conductance and poor agreement with theory. However, it was found that values of $V\Omega g_{NS}(0)/I$ computed separately for each sample were in good agreement for given values of T and V_{inj} . It therefore appears that the quality of the probe junction is not a vital factor in the determination of the quasiparticle potential.

Also included in Fig. 6 is the average conductance of samples 11 for which the Sn was not oxidized: the probe consisted of a Sn-CuAl-Pb (SNS) junction.³⁷ The conductance was independent of temperature except

near T_c , where it decreased. This decrease in conductance was due to the excess boundary resistance at the Sn-CuAl interface discovered by Pippard et al.¹ Since the measurements of the quasiparticle potential V are null measurements ($I_p = 0$), the normalized conductance used in Eq. (11) should not include this conductance dip. The probe junctions on the oxidized Sn samples exhibited a similar but much smaller conductance dip for the same reason. Thus the conductances for these junctions were normalized to the maximum observed conductance (at a temperature somewhat below T_c).

4.3 Determination of τ_Q

At high injection voltages F approaches unity and Eq. (11) becomes

$$\frac{V}{I} \approx \left(\frac{Q}{Q}\right)^* \frac{\tau_Q}{2N(0)e^2\Omega_{NS}(0)}. \quad (eV_{inj} \gg \Delta(T)). \quad (18)$$

In this section, we discuss measurements of V/I for which $eV_{inj} > 10 \Delta(T)$ implying that $F > 0.9$ (see Fig. 4a).

At each temperature V was plotted continuously vs I for both electron injection and electron extraction. From the X-Y recorder traces the values of V/I for $eV_{inj} \approx 10 \Delta(T)$ were determined. For electron injection into the superconductor the CuAl probe was negative relative to μ_p ; for electron extraction it was positive. For all samples the values of V/I for injection and extraction were nearly equal near T_c but showed a gradually increasing asymmetry as the temperature was lowered. In one sample, this asymmetry was as much as 50% at the lowest temperature. Since the excitation spectrum is very nearly symmetric about k_F for $E \ll E_F$, this result, which was also observed by Clarke,⁴ was not expected.

The probe and injection junctions had quite symmetric current-voltage characteristics, and we believe they were not responsible for the observed asymmetry. The average value \bar{V}/I will be used in the data analysis. At low temperatures \bar{V}/I was independent of V_{inj} for values of eV_{inj} greater than $10\Delta(T)$ and less than 30 to 40 $\Delta(T)$ (the highest values studied). Near T_c ($t > 0.98$), V/I increased steadily with increasing injection current I even for $eV_{inj} > 10 \Delta(T)$. This behavior was probably due to a depression in Δ arising from heating in the injection junction. The measured value of \bar{V}/I increased rapidly with decreasing temperature at low temperatures as a result of the temperature dependence of $g_{NS}(0)$. This dependence has been removed in Fig. 7 where $g_{NS}(0)\bar{V}/I$ is plotted versus temperature. The quantity $g_{NS}(0)\bar{V}/I$ was computed separately for each sample, and the values then averaged over all acceptable samples of the same thickness. This procedure was also followed for the data plotted on Figs. 8 through 11. We see that $g_{NS}(0)\bar{V}/I$ is inversely proportional to the thickness of the Sn (and hence to the volume Ω) for samples 6, 8, and 15. The measured transition temperature for samples 6 and 8 was 3.81K, and that for sample 15 was 3.86K.

The results for samples 11, for which the Sn was not oxidized, are also shown in Fig. 7. The proximity effect²⁷ of the CuAl on the Sn modifies the behavior considerably. First, the transition temperature of the sandwich was depressed to 3.43K. Second, $g_{NS}(0)\bar{V}/I$ (which is proportional to τ_Q) is roughly 20 times higher than the value for sample 15, which has a comparable thickness of Sn. It was also observed that the injection junction characteristic showed no observable energy gap down to the transition temperature of the Al at 1.8K. Since τ_Q increases for decreasing Δ for both the inelastic and elastic contributions

[Eqs. (15) and (16)], this dramatic increase in τ_Q is reasonable.

However, we can draw no quantitative conclusions. The injection volume Ω is no longer well defined, as pairs penetrate into the CuAl. In addition, the theory assumed tunneling detection, and it is not clear to what extent the results are correct for a metallic probe with $g_{NS}(0)$ set equal to unity over the entire temperature range. Finally, we have no proper measure of the degree of gaplessness in the Sn. Nevertheless, the qualitative result is interesting, and consistent with our theoretical picture of the processes involved.

In order to determine τ_Q it is convenient to consider the quantity derived from Eq. (11) in the limit $eV_{inj} \gg \Delta$ ($F \approx 1$):

$$\zeta = \bar{v} g_{NS}(0) \Omega / I = \frac{Q^*}{Q} \frac{\tau_Q}{2e^2 N(0)}. \quad (eV_{inj} \gg \Delta). \quad (19)$$

The relaxation processes for the inelastic and elastic contributions to τ_Q are independent, so that $\tau_Q^{-1} = (\tau_Q^{ph})^{-1} + (\tau_Q^{el})^{-1}$. The quantity ζ is plotted vs reduced temperature in Fig. 8 for samples 6, 8, and 15 (clean Sn), and samples 19 (Sn + 3 wt% In). The data for the clean samples have been averaged together. Very close to T_c , all data lie on the same curve: this result implies that the phonon-mediated processes dominate in this temperature region, irrespective of the mean free path of the Sn. At lower temperatures, the data for sample 19 lie above those for the clean samples, implying that τ_Q is longer in the dirty sample: the anisotropy in this sample has been greatly reduced, and the contribution of the elastic scattering to τ_Q has been partly or entirely removed.

We assume for the moment that only the phonon processes contribute to τ_Q for samples 19. The solid line in Fig. 8 represents a fit of $\zeta = 2.3 \times 10^{-14} \Delta(0)/\Delta(T)$ to these data, $\Delta(0)/\Delta(T)$ being the predicted dependence of τ_Q^{ph} near T_c . The fit is excellent above $t = 0.7$, but at lower temperatures the data lie above the curve. If the theory were still strictly valid at lower temperatures, the data should lie below the theoretical curve. Tinkham's estimate of τ_Q^{ph} at low temperatures is roughly 2/3 of the extrapolation of the high temperature value. In addition, Q^*/Q is expected to be less than unity in this temperature range. Our experimental result suggests that the theory is probably rather inaccurate at lower temperatures, as expected. One consequence is that we can deduce nothing experimentally about the value of Q^*/Q .

Using the data for both clean and dirty samples near T_c , the value of $N(0)$ from Table I, and setting $Q^*/Q = 1$, we find from Eq. (19) $\tau_Q^{\text{ph}} = 4.40 \times 10^3 \zeta = 1.0 \times 10^{-10} \Delta(0)/\Delta(T) \text{ sec } (T \sim T_c)$. This value is a factor of three smaller than the corrected preliminary value of Clarke,⁴ and one half of the theoretical estimate. We consider this good agreement between theory and experiment, in view of the various approximations made in the theory.

We can now estimate the contribution of elastic scattering processes to Q -relaxation for the clean samples, and compare the value of τ_Q^{el} with Eq. (16). Sufficiently close to T_c , the cooling time $t(T_c)$ is shorter than $\tau_Q \approx \tau_Q^{\text{ph}}$, and the quasiparticles come into separate thermal equilibrium on each branch before branch mixing. The range of temperature over which $t(T_c) < \tau_Q^{\text{ph}}$ depends critically on the value of $t(T_c)$: if we take the estimate of Eq. (13), the range is $t = T/T_c \gtrsim 0.95$ (see Fig. 12).

In this limit, we would expect T^* ($k_B T^*$ is the mean energy of the quasiparticles) to be close to T_c . The mean free path of the clean samples was strongly size effect limited,⁴² and we assume that the appropriate elastic scattering time/ $\tau_1 = v_F/d$. The average Sn film thickness d was 2800 Å. Taking the value of v_F from Table I and setting³¹ $\langle a^2 \rangle_0 = 0.02$, we have calculated τ_Q^{el} from Eq. (16). We have then estimated $\tau_Q = [(\tau_Q^{ph})^{-1} + (\tau_Q^{el})^{-1}]^{-1}$, with $\tau_Q^{ph} = 1.0 \times 10^{-10} \Delta(0)/\Delta(T)$. The result is shown as a dashed line in Fig. 8. The agreement with the data is remarkably good for $t > 0.8$. It appears that $T^* = T_c$ is an excellent approximation, and that Eq. (16) is a good estimate of τ_Q^{el} over this temperature range.

At lower temperatures the estimate of τ_Q^{el} using $T^* = T_c$ is too low. This result is expected, since the quasiparticles are certainly branch mixing significantly before they reach equilibrium on each branch. The mean energy at which they mix is therefore higher than $k_B T_c$. For $t \lesssim 0.6$, the data indicate that both τ_Q^{ph} and τ_Q^{el} are nearly independent of temperature. We have assumed $\tau_Q^{ph} \approx 1.0 \times 10^{-10}$ sec and used the data to estimate $\tau_Q^{el} = [\tau_Q^{-1} - (\tau_Q^{ph})^{-1}]^{-1} \approx 1.4 \times 10^{-10}$ sec. We have used this value of τ_Q^{el} in Eq. (16) to estimate $T^* = 2T_c$. The behavior of τ_Q with $T^* = 2T_c$ is also shown in Fig. 8. This estimate is very approximate: the value of τ_Q^{ph} is not very accurate for $t < 0.6$, and we have neglected the factor Q^*/Q . Nevertheless, this estimate of T^* seems reasonable: one would certainly expect T^* to increase appreciably as the temperature is lowered from the region in which $t(T_c) < \tau_Q$ to one in which $t(T_c) > \tau_Q$. This increase takes place as t is decreased from about 0.8 to about 0.6. Eq. (16) appears to be a good estimate of τ_Q^{el} ; however, a much more

careful study would be required to test the mean free path dependence.

We have calculated the contribution of the elastic scattering to τ_Q for the dirty sample. Using $\ell \approx 420 \text{ \AA}$ and $T^* = 2T_c$ we find $\tau_Q^{el} \approx 10^{-9}$ sec. The contribution of the elastic scattering for the dirty Sn was therefore about 10% of the phonon scattering contribution for the lower temperatures.

Finally, we examine the validity of the assumption $w \gg \lambda_Q \gg d$. Most of the injected quasiparticles cross to the far side of the Sn film without scattering in a time $\sim d/v_F \sim 4 \times 10^{-13}$ sec, which is much less than the smallest value of τ_Q . Thus $\lambda_Q \gg d$, and branch mixing occurs uniformly across the film. Quasiparticles diffuse along the film with an elastic mean free path $\sim d$, so that $\lambda_Q \sim (dv_F \tau_Q / 3)^{1/2} \sim 10 \text{ \mu m}$ for the longest value of τ_Q observed, about 10^{-9} sec. Thus $\lambda_Q \ll w \sim 3 \text{ mm}$, and the non-equilibrium volume is closely equal to $w^2 d$.

4.4 The Voltage and Temperature Dependence of F

At high voltages ($eV_{inj} \gg \Delta$) the quantity \bar{V}/I is determined by τ_Q and Q^*/Q . As eV_{inj} is reduced, the degree of branch imbalance produced per unit injection current is also reduced. We then have

$$\zeta = \frac{F(Q^*/Q)\tau_Q}{2e^2 N(0)} = F(V_{inj}, T)\zeta_\infty, \quad (20)$$

where ζ_∞ is the limiting value of ζ for $eV_{inj} \gg \Delta$. We have neglected the fact that Q^*/Q depends somewhat on V_{inj} . Figs. 9 and 10 compare the experimental values of ζ/ζ_∞ with F for samples 10C and 15A. In each case ζ/ζ_∞ was normalized at $eV_{inj}/\Delta(0) = 40$. (In Fig. 10, the Al injection film was superconducting for $t = 0.35$, and we have not included the

theoretical curve for this temperature. The primary effect of the Al gap is to increase the energy gap in the injection current-voltage characteristic to $\Delta_{\text{Sn}} + \Delta_{\text{Al}}$.) The agreement between ζ/ζ_{∞} and F is only fair. However, at low reduced temperatures the value of ζ/ζ_{∞} drops rapidly as eV_{inj} is lowered towards $\Delta(0)$. This drop clearly demonstrates the decrease in branch imbalance per unit current created by electron injection or extraction near the energy gap, compared with the degree of imbalance created for $eV_{\text{inj}} \gg \Delta$.

For the lower reduced temperatures, ζ/ζ_{∞} is too low for $eV_{\text{inj}}/\Delta(0) \lesssim 2$, and too high for $eV_{\text{inj}}/\Delta(0) \gtrsim 2$. It is possible that these discrepancies are due to the quasiparticle interference first observed in thin superconducting films by Tomasch,⁴³ and explained by McMillan and Anderson.³⁴ In this process, an injected $k_{>}$ quasiparticle is reflected at the far side of the superconducting film as a $k_{<}$ quasiparticle (i.e. branch mixing occurs), and the two quasiparticles interfere. This interference is energy dependent, and gives rise to structure on the current-voltage characteristic of the injection junction. Since the reflection involves branch mixing, we might expect to observe structure in a plot of quasiparticle voltage vs injection voltage. The structure should have extrema (maxima or minima depending on the sign of the perturbation in $\Delta(T)$ at the far side of the superconducting film) when³⁴ $\{[eV_{\text{inj}}/\Delta(T)]^2 - 1\}^{1/2} = m\pi^2 \xi(T)/d$, where d is the film thickness, $\xi(T)$ the coherence length, and m an integer. For $\xi(T) \gtrsim d$ or large values of m , this structure has a nearly constant period of $\pi^2 \xi(T)/d$. At low temperatures in Sn, this periodicity is $eV_{\text{inj}} \sim 6.5\Delta(0)$ for $d \sim 3500 \text{ \AA}$. This period is at least suggestive of the structure in Figs. 9 and 10. It is therefore

possible that branch mixing from spatial inhomogeneities in $\Delta(T)$ occurs in our clean films. In order to test this hypothesis properly, it would be necessary to take data from samples in which d was varied over a wide range.

5. EXPERIMENTAL RESULTS: Pb

Preliminary measurements were also made of the quasiparticle potential in Pb for temperatures from 1.3 to 4.2K. The experimental arrangement was identical to that used in the Sn measurements.

5.1 Injection Junctions

The Al-AlOx-Pb junctions had normal state resistances of 1 to 2 Ω and were of very high quality. Their conductances below the gap agreed closely with the theoretical predictions with $T_c = 7.2K$. The Pb phonon structure was also clearly visible on the dV/dI characteristics.

5.2. Probe Junction

The Pb-PbOx-CuAl-Pb junctions had resistances of $\sim 5 \times 10^{-6} \Omega$ at 4.2K, about an order of magnitude higher than that expected for the CuAl barriers alone. These probe junctions were very poor quality tunnel junctions, as their resistances increased by only about 5% as the temperature was lowered from 4.2K to 1.3K. However, the results for Sn indicated that the values of the quasiparticle voltage were not very sensitive to the quality of the probe tunnel junction, provided there was an oxide layer between the Sn and the CuAl to quench the proximity effect. It is likely therefore that the results presented here for Pb were not affected significantly by the proximity of the CuAl. Additional measurements with better probe tunnel junctions would be desirable.

5.3 Comparison with Theory

The values of the quasiparticle voltage per unit current (V/I) for the Pb samples showed only a few percent of asymmetry and were essentially constant for $eV_{inj} > 5\Delta(0)$. The quantity $\zeta = (\bar{V}/I)g_{NS}(0)\Omega$ for both sets of samples is plotted vs reduced temperature in Fig. 11. A smooth curve has been drawn through the data. For samples 12, we used a copper standard resistor, while for samples 16, we used a manganin standard. The large error bars on the data for samples 16 above the λ -point ($t = 0.3$) reflect the high level of thermoelectric noise developed by the manganin (see Section 3.3).

The rise in ζ as the temperature is lowered is inconsistent with the theoretical predictions for τ_Q : both τ_Q^{ph} and τ_Q^{el} should remain roughly constant over this temperature range. At 4.2K, the characteristic time estimated from ζ is about 3×10^{-12} sec; from Eq. (15) (with the prefactor value replaced by 0.044) we deduce a low temperature/for τ_Q^{ph} of about 4×10^{-12} sec.

It is possible that the observed rise in ζ as the temperature is lowered is attributable to the poor quality of the probe junctions. However, no such rise was observed for Sn samples 11, for which there was no oxide barrier between the Sn and the CuAl (see Fig. 7). Alternatively, it may be that quasiparticle recombination is primarily responsible for the relaxation of Q when $t > 0.3$, and that $\tau_Q < \tau_R$ only when $t \lesssim 0.3$. If the value of ζ for $t \lesssim 0.3$ represents τ_Q^{ph} , the required value of τ_Q^{ph} is about 1.6×10^{-11} sec, roughly four times the theoretical estimate. It is not inconceivable that the theory underestimates τ_Q^{ph} by this factor. If we take the theoretical value of Rothwarf and Cohen²³

$$\tau_R = 3 \times 10^{-13} T^{-1/2} \exp(\Delta/k_B T) \text{ sec},$$

we find that τ_R falls below

1.6×10^{-11} sec for $t \gtrsim 0.45$. If we bear in mind the uncertainties in the numerical values, it seems plausible that the temperature dependence of ζ reflects a contribution from recombination processes for $t \gtrsim 0.3$. However, the observed temperature dependence is far from that expected for τ_R .

Structure was observed on plots of quasiparticle voltage against injection voltage. Several oscillations were visible, and we again tentatively ascribe this behavior to quasiparticle interference arising from branch mixing at the Pb surfaces. At low temperatures, the period in $eV_{inj}/\Delta(0)$ was close to $\pi^2 \xi(T)/d$.

6. SUMMARY AND DISCUSSION

In general, the quasiparticles injected into a superconductor from a normal metal via a tunnel junction do not uniformly populate the $k_>$ and $k_<$ branches, but rather generate an imbalance $Q = n_> - n_<$ [see Eq. (6)]. This imbalance relaxes with a characteristic time τ_Q . In the presence of the imbalance, there exists a quasiparticle potential, V [see Eq. (11)], that differs from the chemical potential of the pairs, μ_p . We have detected V by means of a tunnel junction probe, and deduced values of τ_Q in both Sn and Pb under various experimental conditions.

The most complete data are for Sn. The most accurate value for τ_Q is obtained for $eV_{inj} \gg \Delta$ at temperatures close to T_c ($t \gtrsim 0.7$). In these limits, Q -relaxation proceeds by inelastic processes only, and V is fairly accurately given by $V = \tau_Q^{ph}/2N(0)e^2\Omega_{NS}^2(0)$. We find experimentally that $\tau_Q^{ph} = 1.0 \times 10^{-10} \Delta(0)/\Delta(T)$ sec, (within perhaps $\pm 20\%$). This value is a factor of 2 lower than the theoretical estimate [Eq. (15)]:

the agreement is considered excellent, in view of the approximations involved in the theory.¹² In the limit of high voltage injection but at lower temperatures, the theory becomes complicated by the introduction of the factor Q^*/Q (≤ 1) into the expression relating V to τ_Q . In addition, elastic scattering processes become important if the energy gap of the Sn is anisotropic. We have largely eliminated the anisotropy effects by dirtying the Sn in one sample. The high temperature/for this sample data are well fitted by $\tau_Q^{\text{ph}} = 1.0 \times 10^{-10} \Delta(0)/\Delta(T)$ sec. At lower temperatures the theoretical curve lies somewhat below the experimental data. The theory predicts that the low temperature value of τ_Q^{ph} should be about 2/3 of the value extrapolated from high temperatures. The fact that Q^*/Q should be less than unity (Tinkham¹² estimates 0.7 to 1.0) should further reduce V and hence the apparent value of τ_Q^{ph} . It therefore appears that the theory is less reliable at low temperatures than near T_c , as expected. We feel that it will be difficult to experimentally measure the value of Q^*/Q .

We have been able to see clearly the effects of elastic scattering in the clean Sn samples, where the gap is anisotropic. The value of τ_Q^{el} at low temperatures, about 1.4×10^{-10} sec, is in good agreement with the theoretical prediction [Eq. (16)], with $T^* \approx 2T_c$. For $t > 0.8$, the data are well represented by Eq. (16) with $T^* \approx T_c$. It would be of interest to measure τ_Q^{el} for a range of mean free paths, to test the theory more thoroughly. The thickness of our clean samples was close to $\pi\xi(0)/2$, the value of the mean free path which minimizes τ_Q^{el} [Eq. (17)]. In a bulk Sn crystal, the elastic contribution to Q-relaxation will be small if the sample is at all clean. For example, in a sample with

$\lambda \sim 10\mu$ (resistance ratio ~ 1000), $\tau_Q^{el} \sim 2 \times 10^{-9}$ sec at low temperatures, 20 times larger than τ_Q^{ph} .

We have also studied the effects of tunnel injection into Sn at voltages close to Δ . The degree of branch imbalance per unit injection current is then greatly reduced. Our results [Figs. (9) and (10)], are in qualitative agreement with the theoretical predictions of Eq. (5).

Our results for branch relaxation in Pb are rather few, and open to question because of the poor quality of the probe tunnel junctions. The observed rise in ζ as the temperature is lowered is not well understood. However, it is certain that $\tau_R < \tau_Q$ for a substantial range of temperatures. It is therefore possible that the rise in ζ indicates that recombination processes dominate Q-relaxation in Pb down to $t \sim 0.3$. One of us (JLP) plans further measurement of ζ over the temperature range $t = 0.2$ to 1, hopefully with better quality probe junctions. The temperature dependence of ζ should indicate clearly whether τ_R or τ_Q is involved. It might also be noted that it is τ_R rather than τ_R^{eff} which enters here because the phonons generated by recombination excite quasiparticles that populate the two branches equally. Consequently, measurements of the quasiparticle potential in Pb might eventually prove to be a very useful technique for determining τ_R .

In Fig. (12) we have summarized our estimates for τ_Q^{ph} , τ_R , and $t(T_c)$ (the time for injected quasiparticles to cool down to a temperature T_c) as functions of temperature for Sn and Pb. For τ_Q^{ph} (Sn), we have assumed that our high temperature value can be extrapolated to the lower temperatures. τ_Q^{ph} (Pb) was calculated from Eq. (15). We have used Parker's estimate²² for τ_R^{eff} (Sn) and the theoretical estimate²³ for τ_R (Pb) for $t \lesssim 0.9$.

The behavior of τ_R in both cases for $0.9 < t < 1$ (shown dashed) is a guess based on the results for Al in this region.^{14,18} The values for $t(T_c)$ are from Eq. (13), and should increase somewhat near T_c . are very approximate, / Thus it is impossible to estimate realistically the temperature ranges for Sn and Pb for which $\tau_Q^{ph} > t(T_c)$; only in this limit can we assume that the two quasi-particle branches reach equilibrium separately before significant branch mixing occurs. For Sn, τ_Q^{ph} is always much smaller than τ_R . However, for Pb, it appears that τ_R is less than τ_Q^{ph} for $t \geq 0.4$. It is hoped that the implications of this result for branch mixing will soon become clear.

There are two other questions raised by our experiments which might be studied in greater depth. The first concerns the values of τ_Q when the superconductor is quasigapless. Our preliminary result, obtained when the probe was in good metallic contact with the superconductor, indicated that τ_Q was increased by roughly a factor of 20. A substantial increase is predicted for both τ_Q^{ph} [Eq. (15)] and τ_Q^{el} [Eq. (16)] when the energy gap becomes small. It would be of interest to study samples (using a tunneling probe) in which the superconductor was made gapless by the addition of magnetic impurities. The second question concerns the role of elastic scattering at the surfaces of the superconductor, where Δ is spatially non-uniform and branch mixing is known to occur.^{34,43} It is likely that the observed structure on plots of ζ vs V_{inj} arises from such processes. However, we have little feeling for size of the contribution of these processes, and further study is merited.

Finally, we mention an implication of this work in the measurement⁴⁴ of e/h using the Josephson effect. In this experiment, microwaves at

a frequency ω generate constant voltage steps whenever $n\hbar\omega = 2\Delta\mu_p$ (n is an integer). If the voltage and current leads (which are normal metals) on one side (or both sides) of the junction are within a distance λ_Q , the quasiparticle voltage measured by the voltage leads will differ from $2\Delta\mu_p/e$, and a significant error in the value of e/h will result. (Josephson⁴⁵ pointed out that non-equilibrium conditions would modify the chemical potential.) It is certainly possible to make junctions in which such errors could be observed, but in all published determinations of e/h , the current and voltage leads were well separated, and the errors due to non-equilibrium effects utterly negligible.

7. ACKNOWLEDGEMENTS

The initial theoretical work was carried out while one of us (J.C.) was on leave at the Cavendish Laboratory, Cambridge, England. This author would like to thank Professor A. B. Pippard, Dr. J. R. Waldram, Dr. C. J. Adkins, and Dr. B. D. Josephson for numerous profitable discussions. He is particularly grateful to Professor M. Tinkham, with whom he enjoyed detailed discussions over a protracted period, and who was responsible for the development of most of the theory. Professor W. H. Parker kindly allowed us to quote his preliminary results for τ_R in Sn and Pb prior to publication. We thank Richard F. Voss, who calculated the theoretical curves in Figs. 4, 9, and 10.

References and Footnotes

1. A. B. Pippard, F.R.S., J. G. Shepherd, and D. A. Tindall, Proc. Roy. Soc. Lond. A324, 17 (1971).
2. L. R. Testardi, Phys. Rev. B4, 2189 (1971).
3. M. L. Yu and J. E. Mercereau, Phys. Rev. Letters 28, 1117 (1972).
4. J. Clarke, Phys. Rev. Letters 28, 1363 (1972).
5. J. Clarke and S. M. Freake, Phys. Rev. Letters 29, 588 (1972).
6. W. H. Parker and W. D. Williams, Phys. Rev. Letters 29, 924 (1972).
7. R. Peters and H. Meissner, Phys. Rev. Letters 30, 965 (1973).
8. S. Putterman and R. de Bruyn Ouboter, Phys. Rev. Letters 24, 50 (1970).
9. T. J. Rieger, D. J. Scalapino, and J. E. Mercereau, Phys. Rev. Letters 27, 1787 (1971).
10. M. Tinkham and J. Clarke, Phys. Rev. Letters 28, 1366 (1972).
11. C. S. Owen and D. J. Scalapino, Phys. Rev. Letters 28, 1559 (1972).
12. M. Tinkham, Phys. Rev. B6, 1747 (1972).
13. J. Bardeen, L. N. Cooper, and J. R. Schrieffer, Phys. Rev. 108, 1175 (1957).
14. B. I. Miller and A. H. Dayem, Phys. Rev. Letters 18, 1000 (1967).
15. A. Rothwarf and B. N. Taylor, Phys. Rev. Letters 19, 27 (1967).
16. B. N. Taylor, Ph.D. Thesis, University of Pennsylvania (1963).
17. J. L. Levine and S. Y. Hsieh, Phys. Rev. Letters 20, 994 (1968).
18. K. E. Gray, A. R. Long, and C. J. Adkins, Phil. Mag. 20, 273 (1969).
19. As we shall see presently, tunnel injection creates a branch imbalance ($n_{>} \neq n_{<}$) as well as an excess quasiparticle population. However, this type of measurement is relatively insensitive to branch imbalance, and only the excess population is detected.
20. W. Eisenmenger, Tunneling Phenomena in Solids, E. Burstein and S. Lundquist, Eds. (Plenum Press, New York, 1964) p. 371.

21. K. E. Gray, *Phil. Mag.* 20, 267 (1969).
22. W. H. Parker, private communication.
23. A. Rothwarf and M. Cohen, *Phys. Rev.* 130, 1401 (1963).
24. A. F. Andreev, *Zh. Eksp. Teor. Fiz.* 46, 1823 (1964); [*Sov. Phys. JETP* 19, 1228 (1964)].
25. J. Clarke, Proceedings of the 12th International Conference on Low Temperature Physics, Kyoto, Japan, September 4-10, 1970, page 443; J. Clarke, S. M. Freake M. L. Rappaport, and T. L. Thorp, *Solid State Communications* 11, 689 (1972).
26. Owing to a calibration error, the value given in the original letter (ref. 4) was incorrect, and should be multiplied by ~ 0.7 .
27. P. G. de Gennes, *Rev. Mod. Phys.* 36, 225 (1964).
28. For a detailed discussion of tunneling, see J. R. Schrieffer, Theory of Superconductivity (Benjamin, New York, 1964).
29. S. Bermon, Tech. Rep. 1, NSF-GP1100, University of Illinois, Urbana, 1964.
30. W. A. Phillips, *Proc. Roy. Soc.* A309, 259 (1969).
31. D. Markowitz and L. P. Kadanoff, *Phys. Rev.* 131, 563 (1963).
32. P. W. Anderson, *J. Phys. Chem. Solids* 11, 26 (1959).
33. L. T. Claiborne and N. G. Einspruch, *Phys. Rev.* 151, 229 (1966).
34. W. L. McMillan and P. W. Anderson, *Phys. Rev. Letters* 16, 85 (1966).
35. R. P. Giffard, R. A. Webb, and J. C. Wheatley, *Jour. Low Temp. Phys.* 6, 533 (1972).
36. J. Clarke, *Proc. IEEE* 61, 8 (1973).
37. J. Clarke, *Proc. Roy. Soc.* A308, 447 (1969).
38. A. B. Pippard, The Dynamics of Conduction Electrons, (Gordon and Breach, New York, 1965), p. 35.

39. Charles Kittel, Introduction to Solid State Physics, Fourth Edition, (John Wiley and Sons, Inc., New York, 1971), p. 219.
40. R. G. Chambers, Proc. Roy. Soc. 215, 481 (1952).
41. Handbook of Chemistry and Physics, 52nd edition, edited by Robert C. Weast (The Chemical Rubber Co., Cleveland, 1971).
42. The intrinsic mean free path of the Sn was found to be $\sim 8500 \text{ \AA}$ in a separate measurement on a thick film.
43. W. J. Tomasch, Phys. Rev. Letters 15, 672 (1965).
44. W. H. Parker, D. N. Langenberg, A. Denenstein, and B. N. Taylor, Phys. Rev. 177, 639 (1969).
45. B. D. Josephson, Adv. in Phys. 14, 419 (1965).

Table I
Electronic Parameters for Sn and Pb

Quantity	Units	Sn	Pb	Reference
γ	$\text{Jcm}^{-3}\text{K}^{-2}$	1.08×10^{-4}	1.62×10^{-4}	ISSP ³⁹
$N(0)^a$	$(\text{eV})^{-1}\text{cm}^{-3}$	1.39×10^{22}	2.07×10^{22}	---
θ	K	200	105	ISSP ³⁹
σ/ℓ	$\Omega^{-1}\text{cm}^{-2}$	9.5×10^{10}	9.4×10^{10}	Chambers ⁴⁰
v_F^b	cm sec^{-1}	0.65×10^8	0.43×10^8	---
$\rho(293\text{K})$	$\Omega \text{ cm}$	11.5×10^{-6}	22×10^{-6}	CRC Handbook ⁴¹
τ_θ^c	sec	2×10^{-14}	3×10^{-14}	Tinkham ¹²
$\xi(0)^d$	\AA	2350	830	---

^a $N(0)$ is the density of states at the Fermi surface per spin per unit energy per unit volume, calculated from $N(0) = 3\gamma/2\pi^2 k_B^2$, where γ is the coefficient of the electronic specific heat. ^bThe values of the Fermi velocity have been calculated³⁸ from $v_F = \pi^2 k_B^2 \sigma / e^2 \ell \gamma$, where ℓ is the electron mean free path and σ the conductivity. ^c $\tau_\theta (= \ell_\theta / v_F)$ is the scattering time at the Debye temperature θ , extrapolated linearly from the value at 293K. ^d $\xi(0) = 0.18 \hbar v_F / kT_c$.

FIGURE CAPTIONS

Fig. 1. Excitation spectrum of a superconductor with energies referred to μ_p . There are $n_>$ excitations on the $k_>$ branch and $n_<$ on the $k_<$ branch. The imbalance $Q = n_> - n_<$.

Fig. 2. Configuration for observation of quasiparticle imbalance. A current I injects quasiparticles into the non-equilibrium volume Ω of the superconductor S via a tunnel junction. The normal probe N_p measures the quasiparticle potential V .

Fig. 3(a). Tunnel injection of an electron from a normal metal (N) into a superconductor (S) at a bias voltage V . When $E_L + E_R = eV > \Delta$, $u_>^2 > u_<^2$, and the $k_>$ branch has a higher population than the $k_<$ branch.

(b) Tunnel extraction of an electron from S into N . When $E_L + E_R = eV > \Delta$, $v_<^2 > v_>^2$, and the $k_<$ branch is preferentially populated.

Fig. 4(a). Degree of branch imbalance F created by the injection current versus $eV_{inj}/\Delta(T)$ for several values of $\Delta(T)/k_B T$.

(b) The function F versus $eV_{inj}/\Delta(0)$ for values of reduced temperature t corresponding to $\Delta/k_B T$ in (a).

Fig. 5. Experimental configuration for measuring quasiparticle potential. The order of evaporation is: Al, Sn(or Pb), SiO, CuAl, and Pb. The current I ($X'Y'$) generates a quasiparticle potential across YZ . This potential is measured by the superconducting galvanometer (G) in series with a resistance R_{std} in a null-balancing technique.

Fig. 6. Normalized low voltage conductance $g_{NS}(0)$ for the normal probe junctions on the Sn samples versus $\Delta/k_B T$, compared with theory (solid line).

Fig. 7. $(\bar{V}/I)g_{NS}(0)$ versus T for clean Sn samples. In sample 11, there was no oxide barrier between the Sn and the CuAl probe.

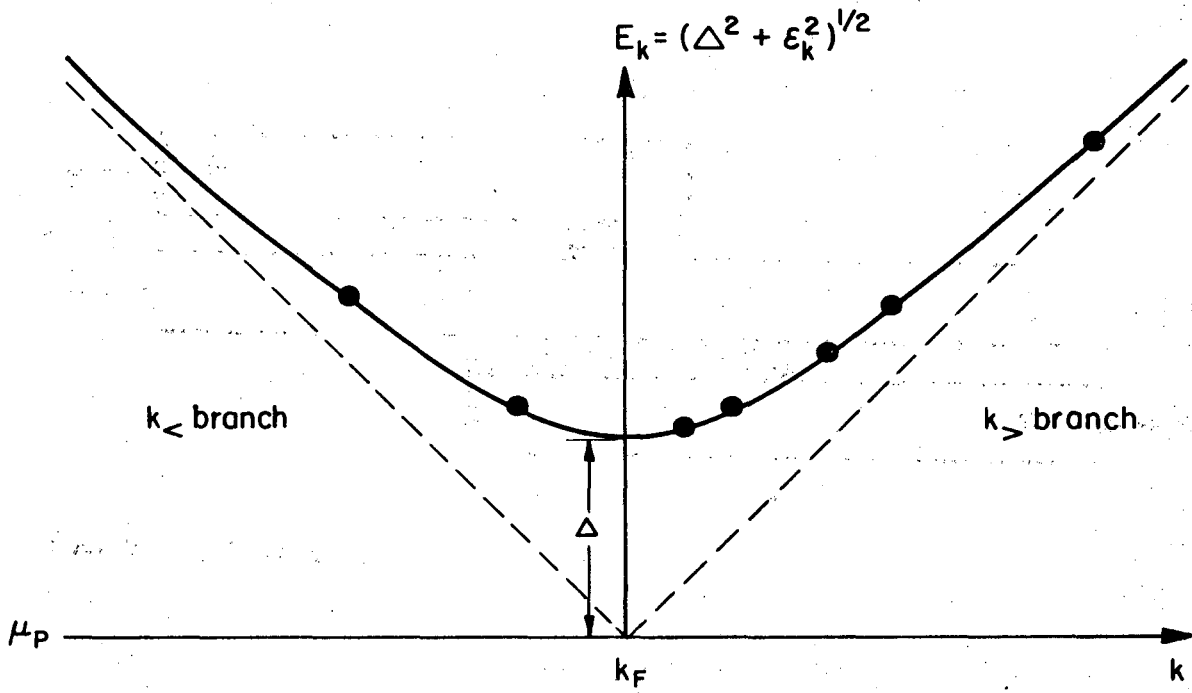
Fig. 8. ζ versus reduced temperature t for clean Sn samples (data averaged over all samples), and for dirty Sn sample 19 (Sn+3 wt.% In). The solid line is a fit to the data for the dirty Sn for $t \gtrsim 0.7$, assuming that only phonon processes contribute. The dashed lines represent both inelastic and elastic contributions: $\tau_Q = (1/\tau_Q^{ph} + 1/\tau_Q^{el})^{-1}$. τ_Q^{el} has been calculated from Eq. (16), using $T^* = T_c$ near T_c , and $T^* = 2T_c$ at low temperatures.

Fig. 9. Sample 10C: ζ/ζ_∞ versus $eV_{inj}/\Delta(0)$ (solid curves) for reduced temperatures $t = 0.53$ and 0.89 ; calculated values of F (dashed curves) for $t = 0, 0.5, 0.9$, and 1.0 .

Fig. 10. Sample 15A: ζ/ζ_∞ versus $eV_{inj}/\Delta(0)$ (solid curves) for $t = 0.35$ and 0.52 ; calculated values of F (dashed curves) for $t = 0, 0.5$, and 1.0 .

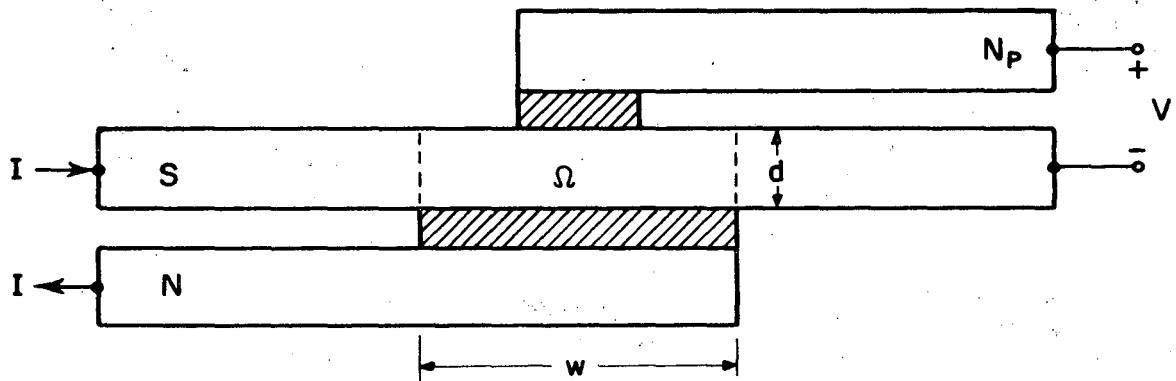
Fig. 11. ζ versus reduced temperature t for Pb samples 12 and 16. A smooth curve has been drawn through the data. The dashed line is the low temperature theoretical estimate of $\zeta = \tau_Q^{ph}/2e^2N(0)$.

Fig. 12. Estimates of τ_Q^{ph} , τ_R , and $t(T_c)$ for Sn and Pb.



XBL 738-1718

Fig. 1



XBL 736-6344

Fig. 2

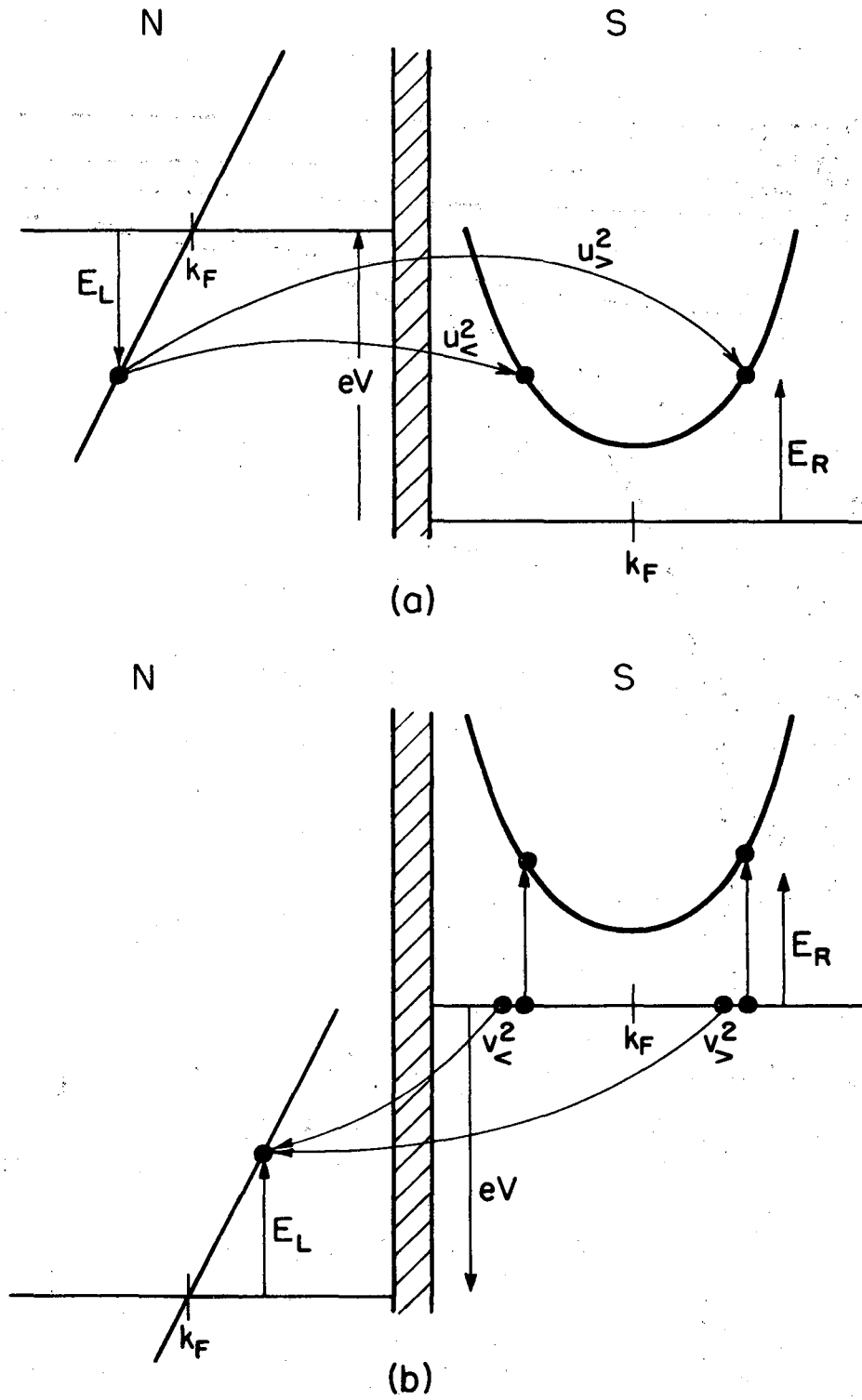
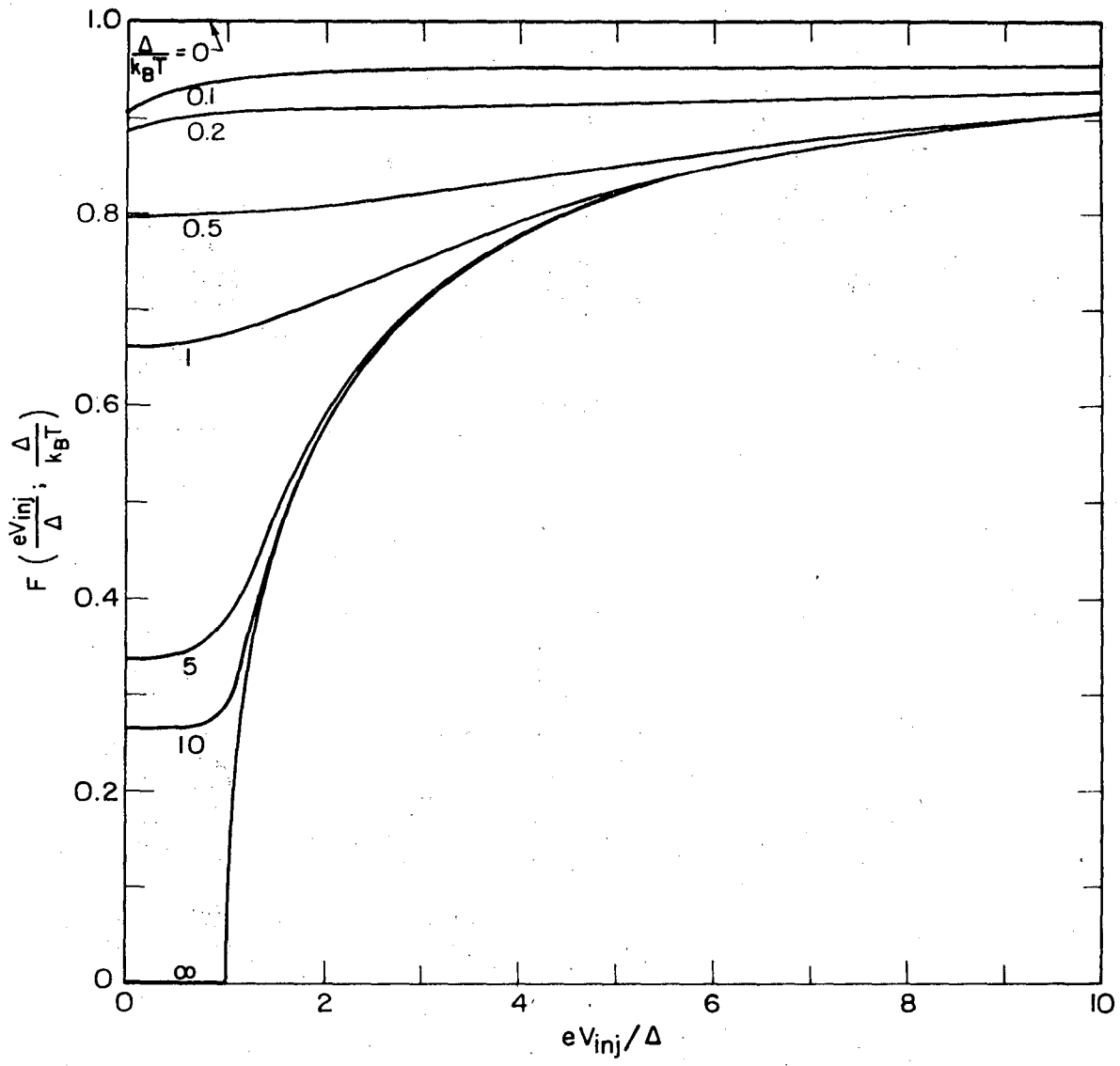


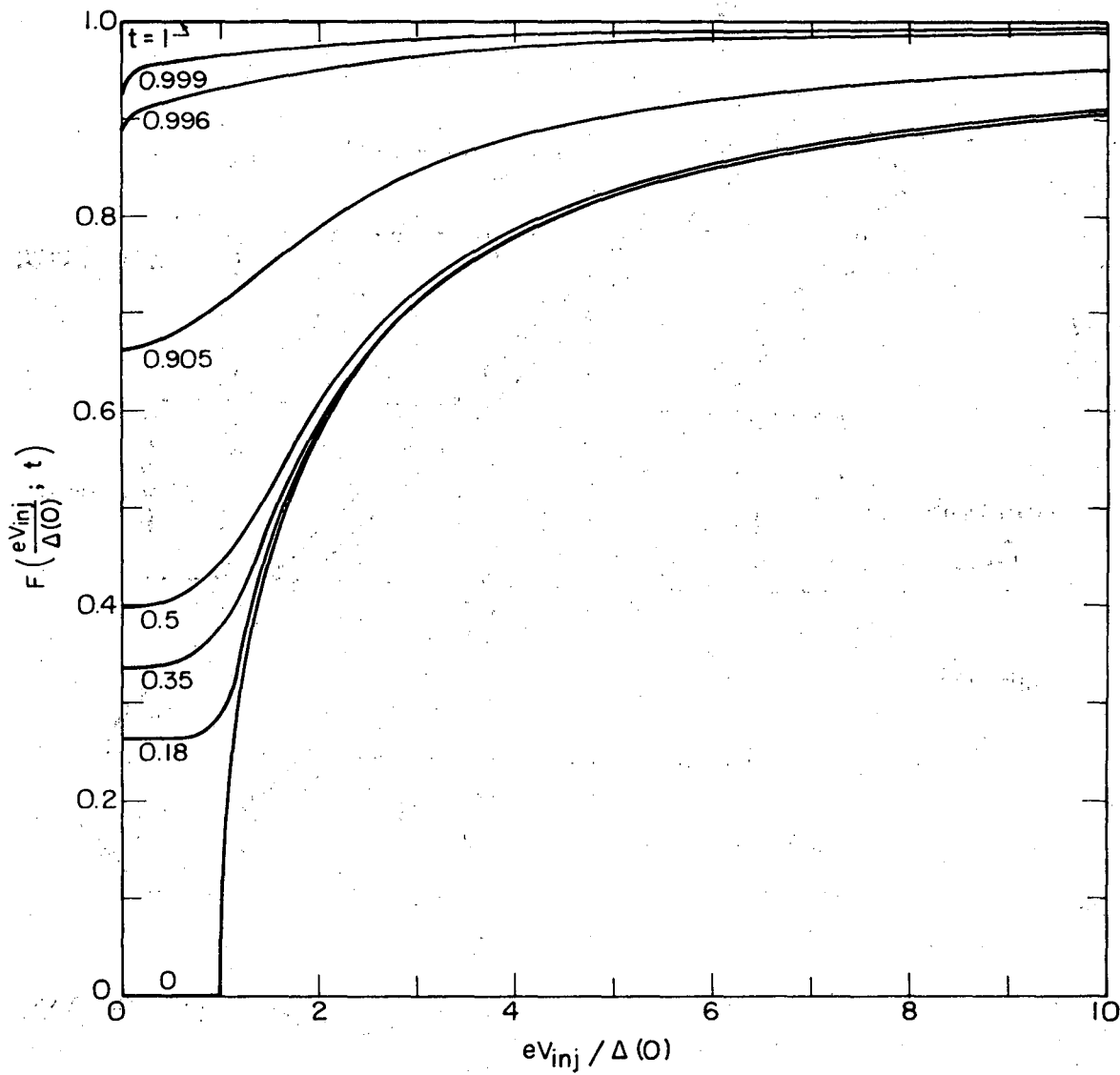
Fig. 3

XBL 736-6346



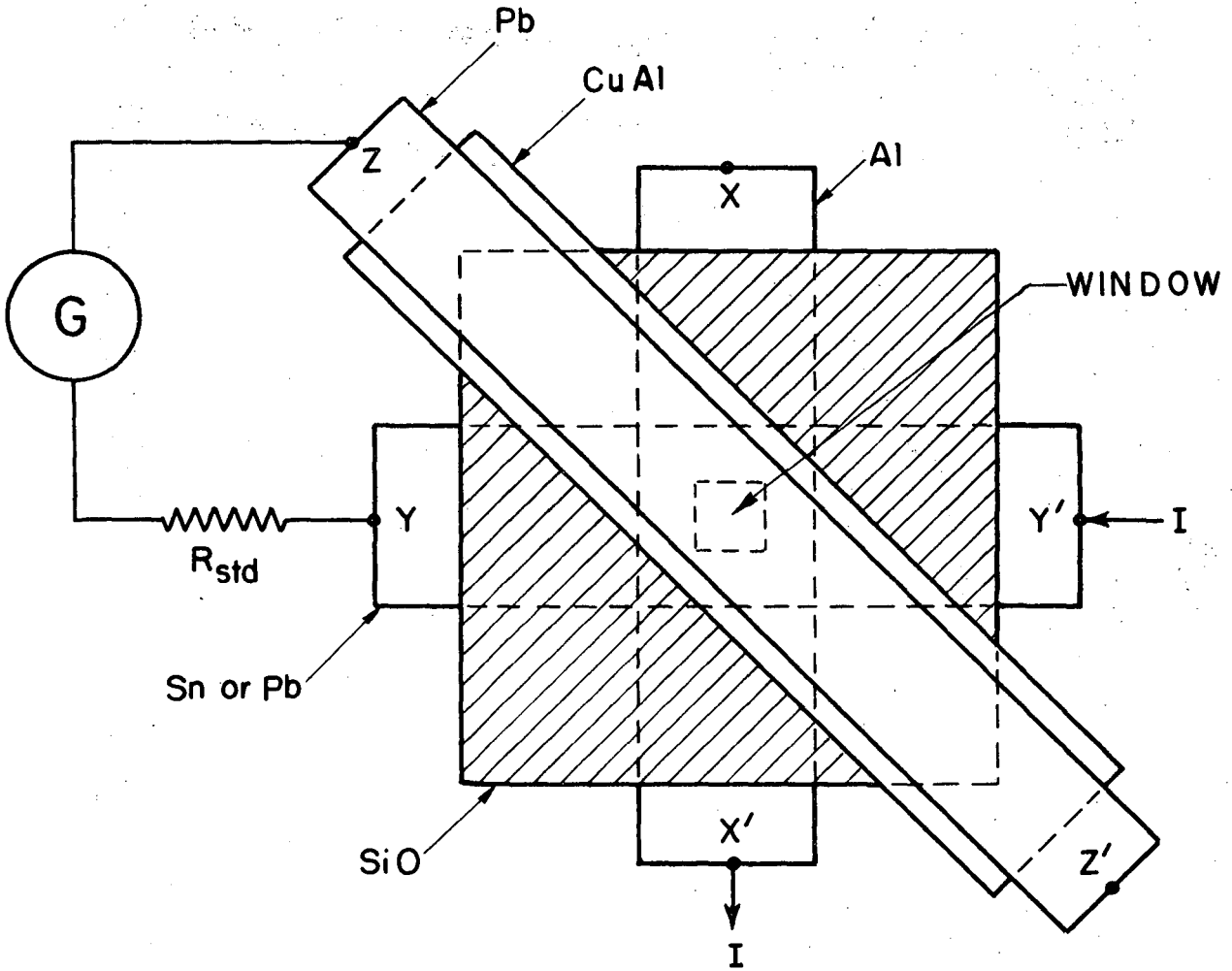
XBL 736-6347

Fig. 4(a)



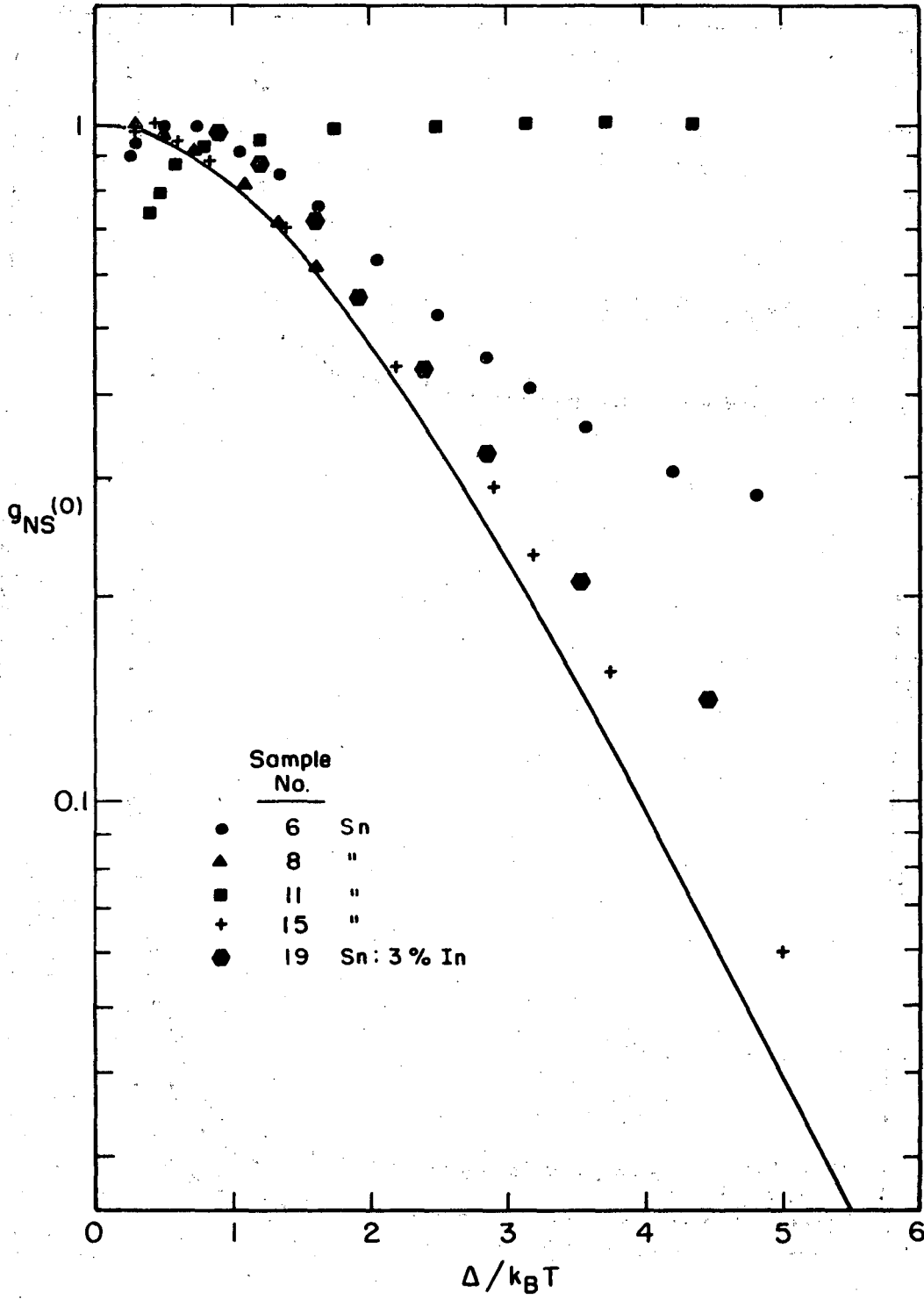
XBL 737-6375

Fig. 4(b)



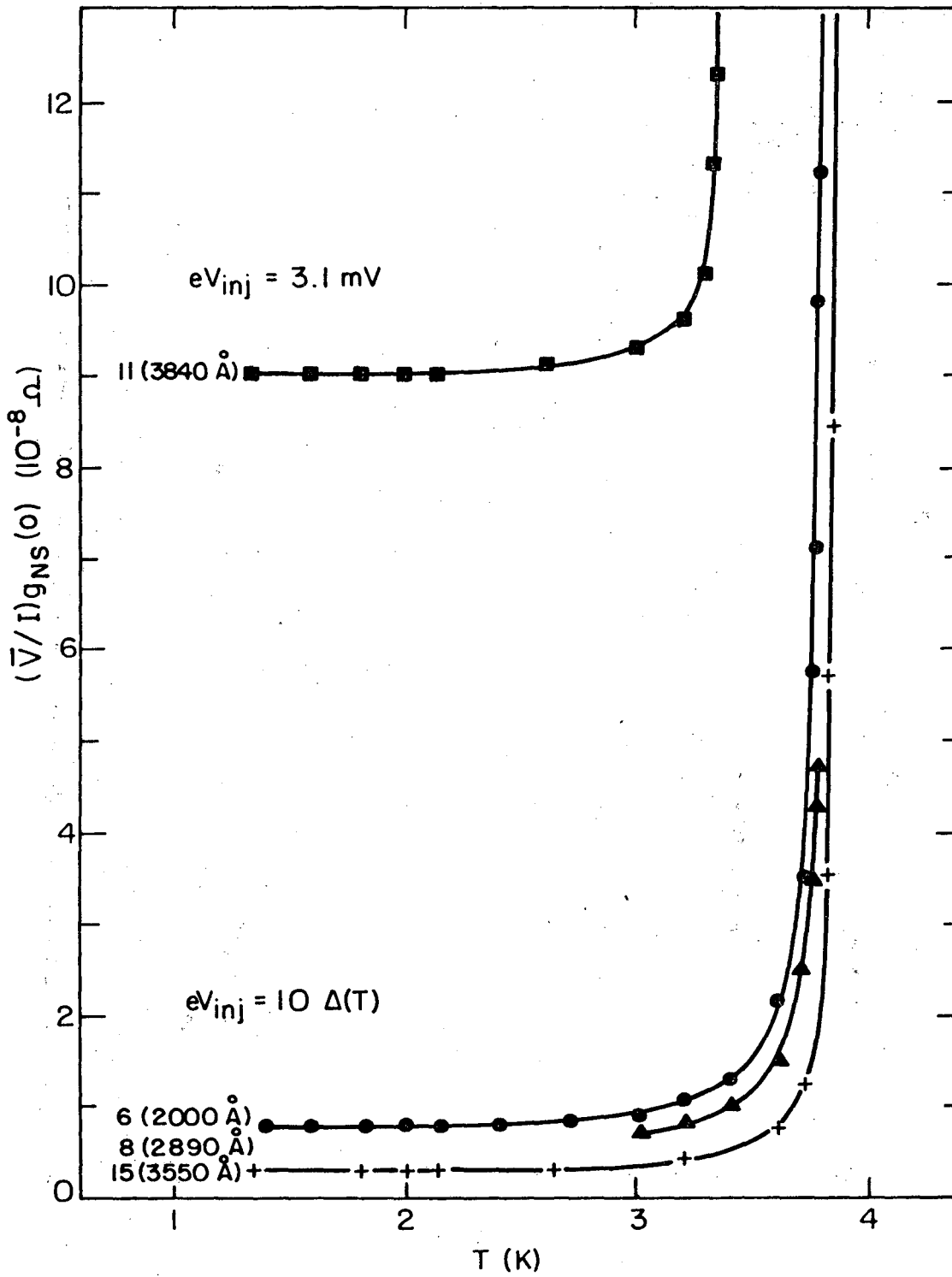
XBL 736-6348

Fig. 5



XBL 736-6353

Fig. 6



XBL736-6354

Fig. 7

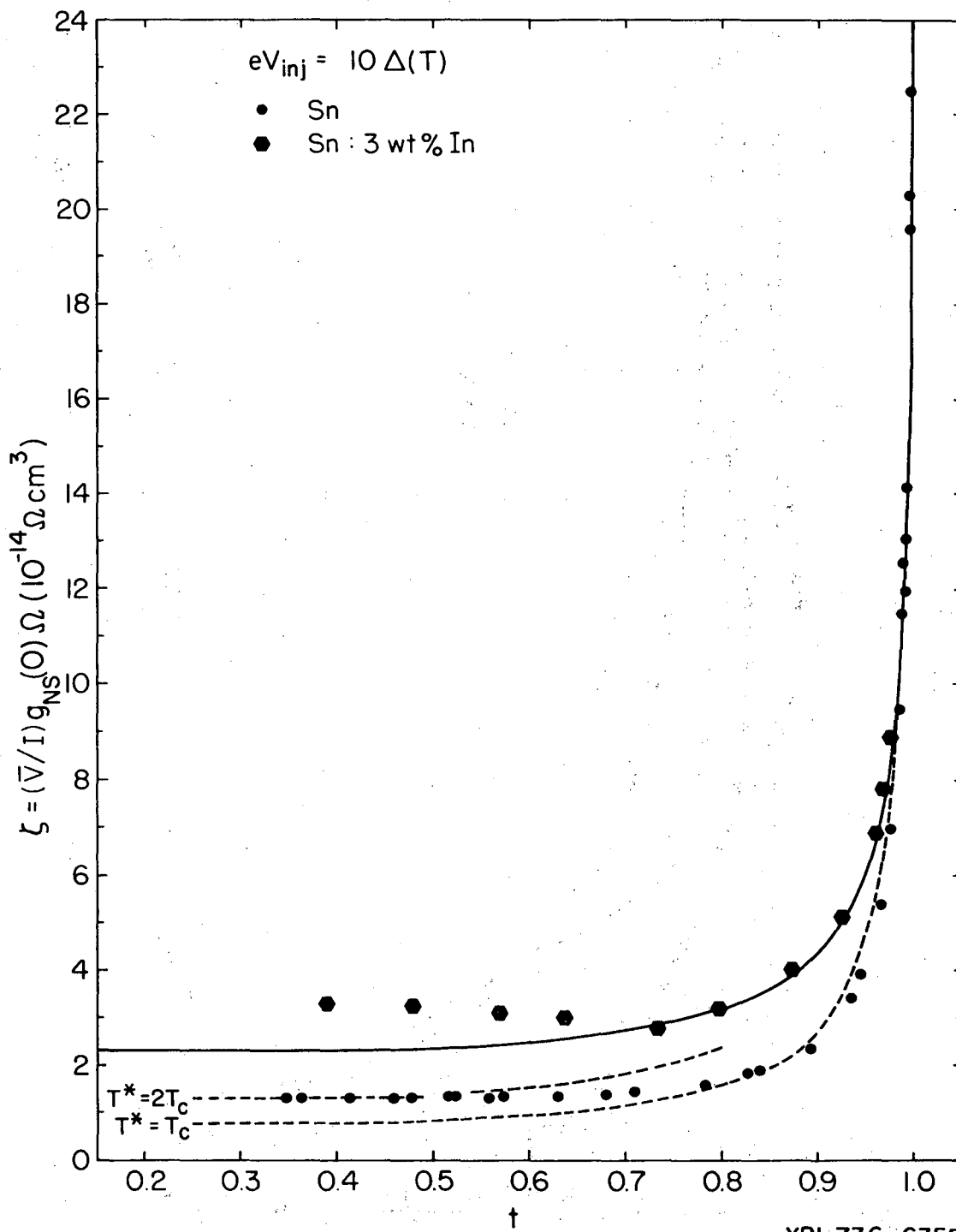
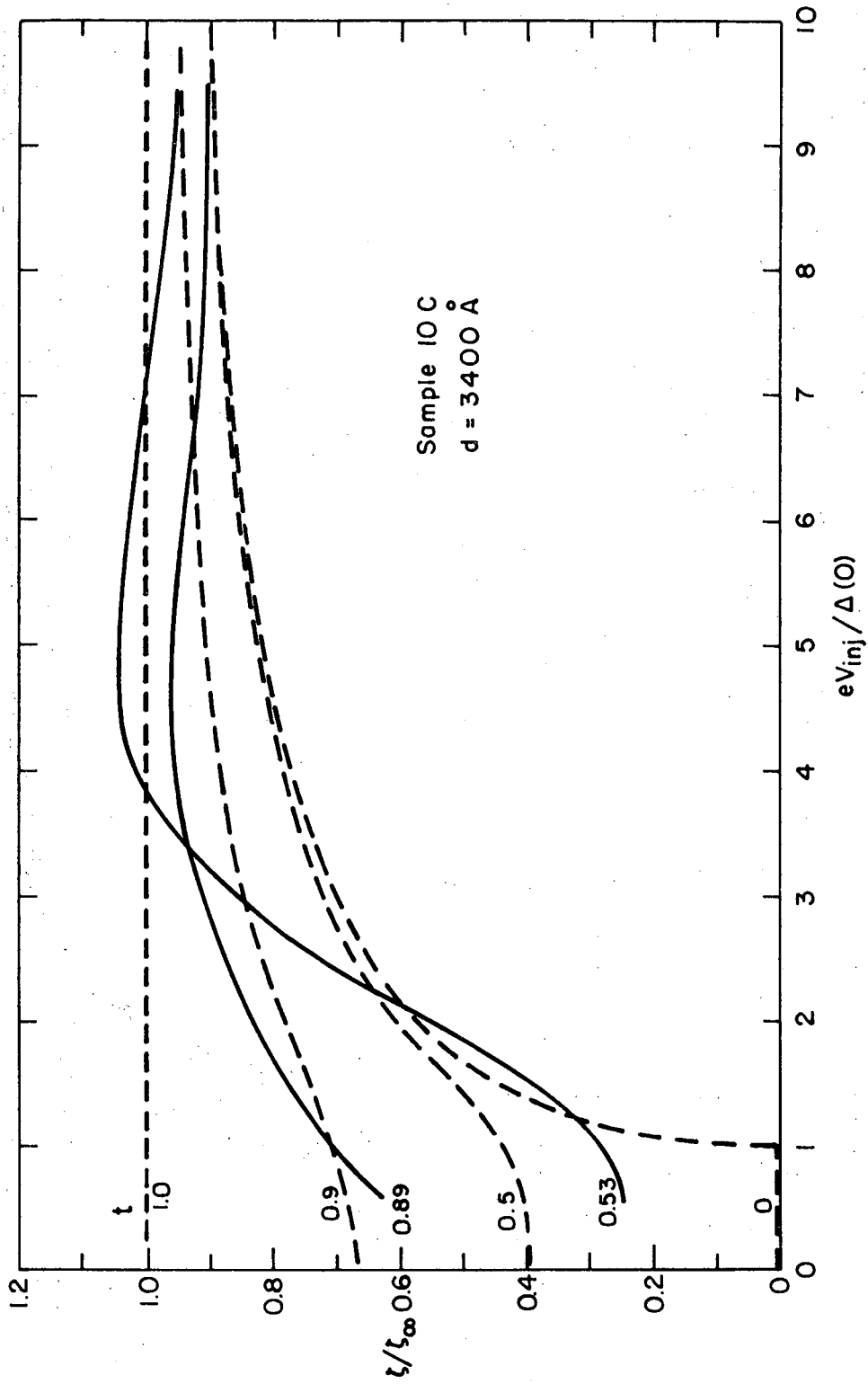
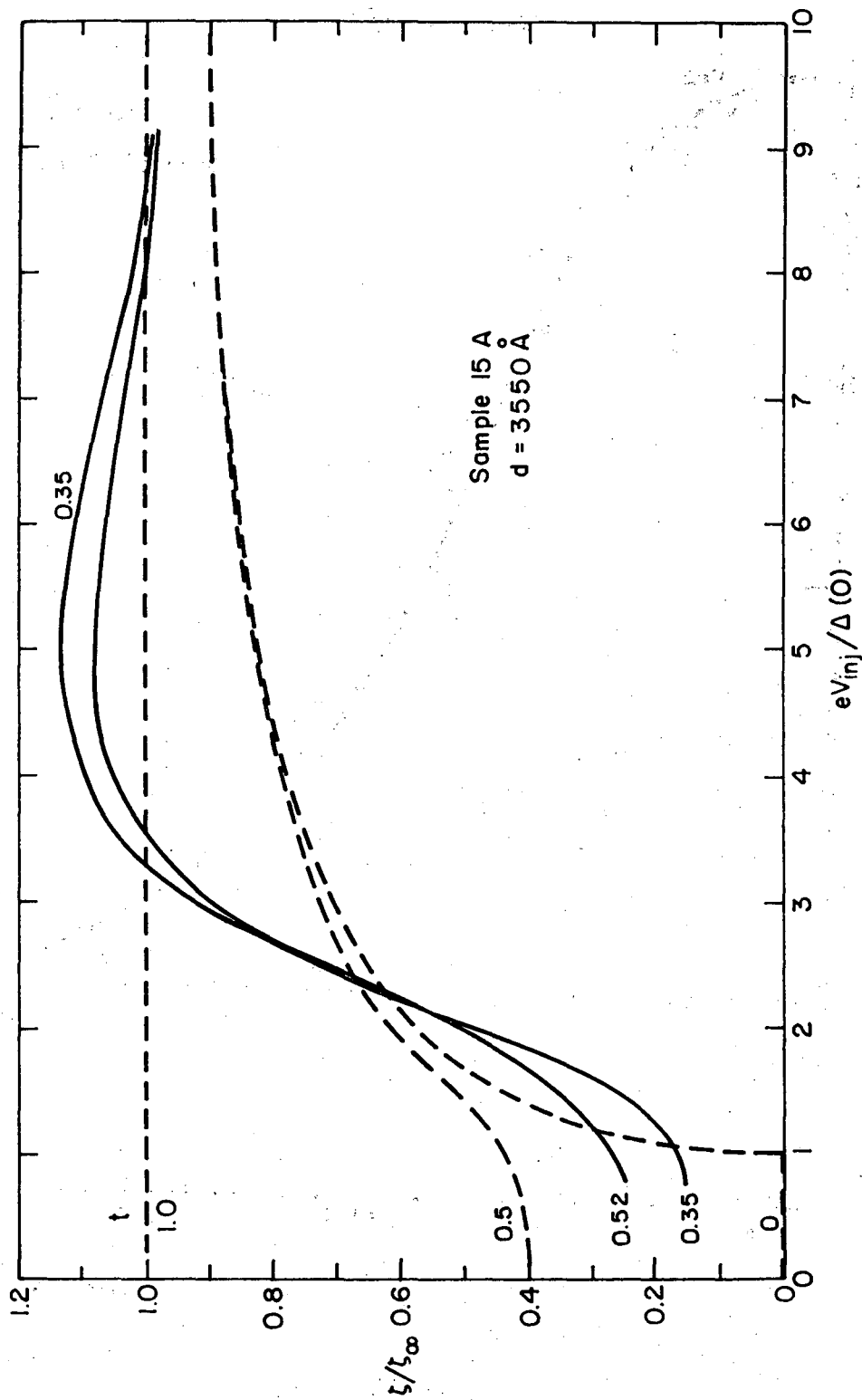


Fig. 8



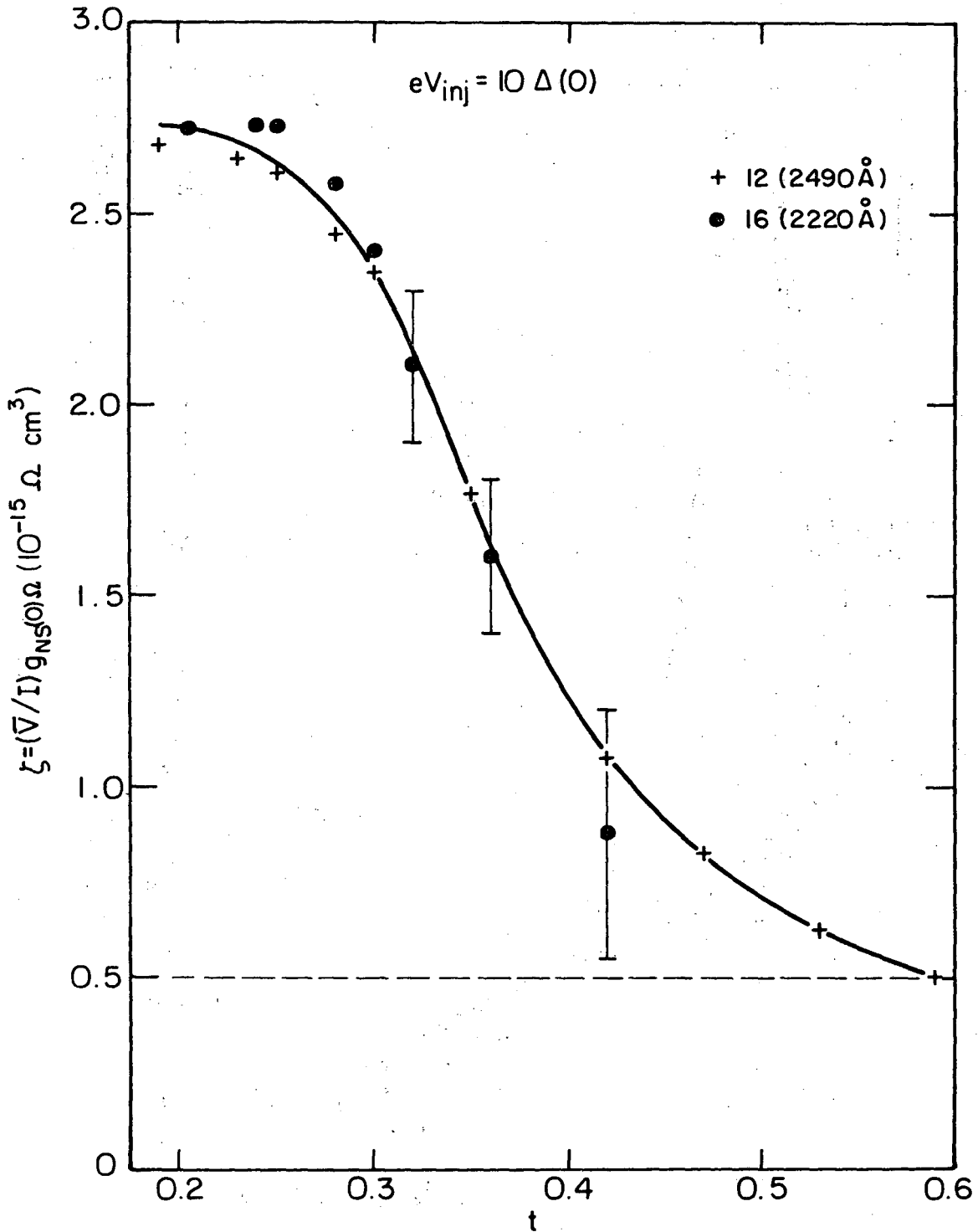
XBL 736-6357

Fig. 9



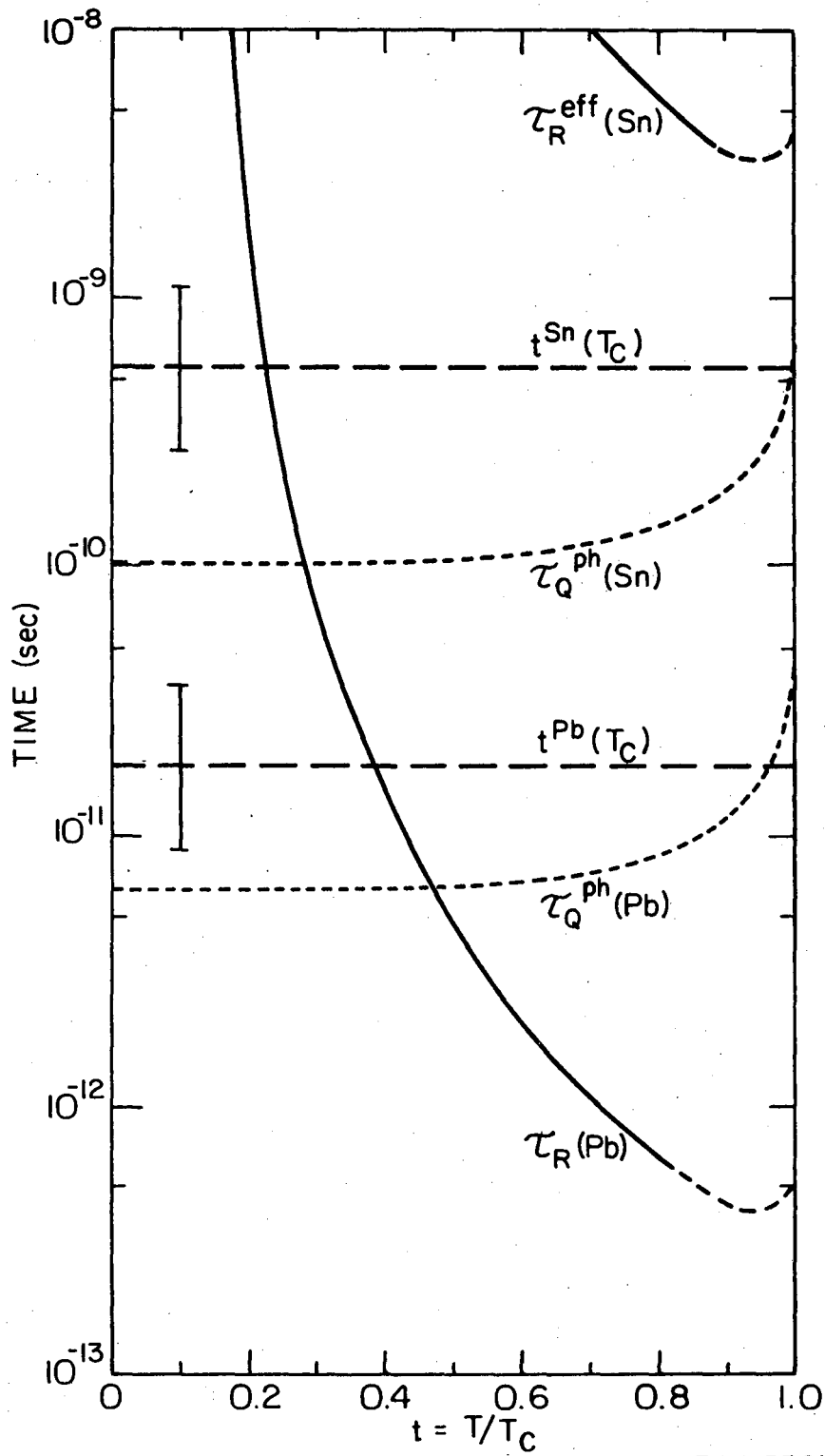
XBL 736-6358

Fig. 10



XBL 736-6363

Fig. 11



XBL7311-5591

Fig. 12

LEGAL NOTICE

This report was prepared as an account of work sponsored by the United States Government. Neither the United States nor the United States Atomic Energy Commission, nor any of their employees, nor any of their contractors, subcontractors, or their employees, makes any warranty, express or implied, or assumes any legal liability or responsibility for the accuracy, completeness or usefulness of any information, apparatus, product or process disclosed, or represents that its use would not infringe privately owned rights.

TECHNICAL INFORMATION DIVISION
LAWRENCE BERKELEY LABORATORY
UNIVERSITY OF CALIFORNIA
BERKELEY, CALIFORNIA 94720